General Disclaimer

One or more of the Following Statements may affect this Document

- This document has been reproduced from the best copy furnished by the organizational source. It is being released in the interest of making available as much information as possible.

- This document may contain data, which exceeds the sheet parameters. It was furnished in this condition by the organizational source and is the best copy available.

- This document may contain tone-on-tone or color graphs, charts and/or pictures, which have been reproduced in black and white.

- This document is paginated as submitted by the original source.

- Portions of this document are not fully legible due to the historical nature of some of the material. However, it is the best reproduction available from the original submission.

NASA TECHNICAL MEMORANDUM

NASA TM X-73545

(NASA-TM-X-73545)   HYBRID COMPOSITES,
STATE-OF-THE-ART REVIEW: ANALYSIS, DESIGN,
APPLICATION AND FABRICATION (NASA)   54 p HC
A04/MF A01   CSCL 11D

N77-18219

Unclas
G3/24   17205

HYBRID COMPOSITES - STATE-OF-THE-ART REVIEW: ANALYSIS; DESIGN, APPLICATION AND FABRICATION

by C. C. Chamis and R. F. Lark
Lewis Research Center
Cleveland, Ohio 44135

MAR 1977
RECEIVED
NASA STI FACILITY
INPUT BRANCH

CONTENTS

E-8980

HYBRID COMPOSITES - STATE-OF-THE-ART REVIEW:
ANALYSIS, DESIGN, APPLICATION AND FABRICATION

by C. C. Chamis and R. F. Lark

Lewis Research Center

ABSTRACT

A state-of-the-art review is presented for hybrid composites that covers the areas of constituents and types of hybrids, analytical methods, design methods, applications, and fabrication procedures. The review summarizes significant contributions in each area and points out areas for further research. The description of each significant contribution is supplemented with pertinent illustrations and references.

Key Words: hybrid composites, interply, intraply, superhybrids, constituents, mechanical behavior, composite mechanics, stress analysis, structural analysis, design, design data, application, fabrication.

INTRODUCTION

Hybrid composites have more than one kind of fiber embedded in the matrix. They have been developed as a structural material as a logical sequel to conventional composites, which have only one kind of fiber. Hybrid composites have unique features that can be used to meet diverse and competing design requirements in a more cost-effective way than either advanced or conventional composites. Some of the specific advantages of hybrids over conventional composites are balanced strength and stiffness, balanced bending and membrane mechanical properties, balanced thermal distortion stability, reduced weight and/or cost, improved fatigue resistance, reduced notch sensitivity, improved fracture toughness and/or crack-arresting properties, and improved impact resistance. By using hybrids, it is possible to obtain a viable compromise between mechanical properties and cost to meet specified design requirements.

Considerable data have been generated for hybrid composites in the areas of analysis, design applications, and fabrication procedures. These data suggest that research in these areas has matured to the point where a state-of-the-art review will provide a valuable source of information for the composites community. It is the objective of this report to provide such a review.

E-8980

This review covers those hybrid composites that consist of two or more different types of fibers (or fiber composites) in a frequently repeated pattern in a laminate. Structural parts that have composites in strategically selected locations or composites that have a few different lamina in strategically selected locations are classified as selectively reinforced components. These types of components are not covered in this review.

The state-of-the-art review presented herein covers constituents and types of hybrids, analytical methods, design methods, applications, and fabrication procedures. Significant contributions in each of these areas are described and are supplemented by pertinent illustrations and references. Over 100 documents were examined. We had to be selective in the inclusion of significant points, illustrations, and references. The amount of material included in the review for each area reflects, to a large extent, the amount of data available in that area. Areas needing further research are pointed out.

We assumed that the reader is familiar with some composite terminology. The few symbols that are used are mostly self-evident and are also defined when they first appear.

CONSTITUENT MATERIALS AND TYPES OF HYBRID COMPOSITES

Fibers

Boron, various types of graphite, glass, and Kevlar fibers are used in hybrid composites. Cloth and fabric woven from these fibers are also used. Typical stress-strain diagrams of some of these fibers are shown in figure 1. As shown in this figure, fibers are available with the following typical ranges of mechanical properties: tensile strength, 250 to 500 ksi (10^3 psi); fracture strain, 0.4 to 4.0 percent; and tensile modulus, 10 to 60 msi (10^6 psi). Fibers are available to meet a variety of diverse or competing design requirements for strength, stiffness, and elongation to fracture.

Resins

The resins used in hybrid composites include mostly structural epoxies. Thermoplastics are now beginning to be used for their improved impact and

moisture-degradation resistance, and polyimides for their elevated-temperature capability and moisture-degradation resistance. The typical stress-strain diagrams of structural epoxies shown in figure 2[1] indicate that epoxies are available with a wide range of properties. However, the intermediate-modulus epoxy is used in most hybrids.

Unidirectional Composites

Unidirectional composites (UDC's) made from preimpregnated fibrous material in tape form (prepreg tape) can be prepared from any of the fibers and the intermediate-modulus epoxies mentioned previously. The UDC's and their mechanical properties, physical properties, and costs are summarized in table 1[2]. Table 1 includes fiber volume ratio, longitudinal (0°) properties (tension and compression), transverse (90°) properties (tension), interlaminar (short beam) shear strength, in-plane (intralaminar) shear properties, flexural properties, ply thickness, and cost in dollars per pound of prepreg tape[2]. Thermal expansion coefficients (TEC) for these UDC's range from slightly negative to about 3×10^6 in./in./°F along the fiber direction and from 15×10^6 to about 30×10^6 in./in./°F transverse to the fiber direction. For thermal expansion coefficients of specific UDC's and the effect of temperature on their mechanical properties, see reference 3. Examining the 0° tension properties in table 1 shows that UDC tensile strengths range from 85 to 230 ksi and their moduli range from 5 to 40 msi. Therefore, suitable combinations of these UDC's may be selected to meet diverse or competing design requirements, as is discussed later.

Types of Hybrids

This review is limited to four general categories of hybrid composites: (1) interply (interspersed or core/shell); (2) intraply; (3) interply/intraply; and (4) superhybrid.

Cross sections of typical hybrids are shown in figures 3 and 4. Briefly, the interply hybrids consist of plies from two or more different UDC's stacked in a specified sequence (fig. 3(a)). Several interply hybrids that were studied by Hoggatt[2] are listed in table 2. This table also shows a notation convention that may be used to define or specify

hybrids. Intraply hybrids consist of two or more different fibers mixed in the same ply (fig. 3(b)). Interply/intraply hybrids consist of plies of intraply and interply hybrids stacked in a specified sequence (fig. 3(c)). Superhybrids consist of resin composite plies, metal composite plies, and metal foils stacked in a specified sequence (fig. 4).

The interply and intraply hybrids generally have the same matrix, and the laminate is fabricated by the cocuring procedure according to specifications provided by the prepreg tape supplier[4]. If the plies for these hybrids are made from different matrices, the hybrid is fabricated by a curing procedure that is compatible with both systems[2,5]. The super-hybrid is fabricated[6] by adhesively bonding metal foils, boron/aluminum (or other metal matrix) UDC plies, and resin/fiber prepreg UDC with an ad-hesive that has the same curing cycle as the prepreg tape[6].

ANALYTICAL METHODS FOR HYBRIDS

The mechanical behavior of hybrid composites is reviewed with respect to stress-strain or load deformation, in-plane and bending (flexural) re-sponse, failure modes, failure criteria, and restrained strains. The review of stress analysis covers methods for determining stress at a point (ply stress) and for determining stress concentrations and also methods associated with fracture mechanics and the postulation of failure criteria. The review of structural analysis summarizes those methods that have been used to predict the structural response of hybrid composite components to static, dynamic, or impact loadings. The environmental, cyclic, and fatigue load effects on the mechanical behavior of hybrids are reviewed in the section DESIGN METHODS.

Mechanical Behavior of Hybrids

Mechanical behavior of unidirectional hybrids. - The observed mechan-ical behavior of hybrids (as of other structural materials) is fundamental in determining which existing methods for predicting mechanical behavior are applicable and in postulating hypotheses for deriving new analytical methods.

Stress-strain diagrams along the fiber (0°) direction for interply unidirectional hybrids are shown in figure 5[4]; those transverse to the

fiber (90°) direction are shown in figure 6[4]. These hybrids consist of three different hybridization (volume) ratios of Modmor II (MOD II) graphite and S-glass (S-GL) fibers in PR-286 epoxy (E). The important observations from figures 5 and 6 are as follows.

1. The stress-strain behavior is linear in both directions.

2. The 0° stress-strain curves of the hybrids lie between the two constituents and are proportional to the amount of constituents (MOD II/ S-GL hybridization ratio).

3. The 0° fracture stresses of the hybrids are less than those of the constituents.

4. The fracture strains of the hybrids appear to be limited to the fracture strain of the graphite (MOD II/E) composite, which is the more brittle constituent in this hybrid.

5. The 90° fracture stress of the hybrids appears to be independent of the hybridization ratio, but the fracture strain decreases proportionately with the hybridization ratio.

Fracture stress variations with the volume percent of graphite in a GY-70-graphite/S-glass hybrid are shown in figure 7[7]. There is an initial rapid drop in both longitudinal fracture stresses (figs. 7(a) and (c)) and then a linear increase with increasing volume percent of graphite fiber. The corresponding moduli increase nonlinearly and lie above the straight line connecting the moduli of the constituents (end points). This apparent "synergistic effect" is the result of stacking the stiffer plies further away from the neutral plane. The transverse tensile strength and modulus (fig. 7(b)) decrease linearly with increasing volume percent of graphite fiber. The shear strength and modulus (fig. 7(d)) decrease approximately linearly with increasing volume percent of graphite fiber. Interesting points to be noted from the curves in figure 7 are (1) the difference in the shear strength and modulus in the two different directions for the graphite composite; and (2) the difference in the shear strength between the short-beam and torsion values for the S-glass composite.

The flexural (bending) strength variation of several interply hybrids,

AS/S-GL and HMS/S-GL, with varying volume percent of S-glass is shown in figure 8[5]. Note (1) the rapid linear drop of the flexural strength of the type AS graphite/S-glass (AS/S-GL) hybrid with increasing volume percent of S-glass; and (2) the approximate linear increase in flexural strength of the high-modulus graphite/S-glass (HMS/S-GL) hybrid with increasing volume percent of S-glass. Observed flexural fracture modes for the HMS/S-GL interply hybrid are illustrated schematically in figure 9[5]. As shown, the interply hybrids may exhibit several peak stresses before fracture and thereby provide increased energy absorption capability of the more brittle constituent.

Flexural strengths for several hybrids are shown in figure 10[5]. The flexural strength data fall below the straight line connecting the strengths of the constituents (end points). Also, the flexural strength of the HMS/S-GL intraply hybrids appears to be independent of (or at most slightly dependent on) the volume percent of S-glass. Photomicrographs of fracture surfaces showing flexural fracture modes for interply and intraply hybrids are presented in figure 11[5]. Note the staggered fracture surface in the intraply hybrids and the relatively flat fracture surface in the interply hybrid. The staggered fracture surface usually is associated with an increased load-carrying capacity of the hybrid.

The variation of the flexural moduli of various hybrids with the volume percent of S-glass is shown in figure 12[5]. Here too, the data fall below the straight line connecting the moduli of the constituents (end points).

Longitudinal and transverse tensile stress-strain diagrams for super-hybrids and their constituents are shown in figure 13[6]. Figure 13 indicates (1) that the stress-strain diagrams of the superhybrids are linear along the fiber direction and fracture is limited by the fracture strain of the boron/aluminum (B/Al) composite and (2) that the corresponding stress-strain diagrams in the transverse direction are nonlinear, with transverse fracture strains approaching 1 percent.

In summary, the previous observations and discussion on the mechanical behavior of unidirectional hybrids lead to the following important

conclusions:

1. The in-plane stress-strain behavior to fracture is approximately linear in general.

2. The data for fracture stresses, for both in-plane and flexure, fall below the straight line connecting the corresponding strengths of the constituents (end points). This indicates some loss in efficiency of property translation relative to the constituent composites.

3. The flexural moduli of interply hybrids depend on the stacking sequence of the constituents.

Mechanical behavior of off-axis hybrids. - We are not aware that any data have been reported on off-axis (unidirectional hybrids loaded other than 0° to the fiber direction) properties of hybrids. These data would be useful in two important respects: (1) to verify the transformation equations for elastic constants (normal moduli, Poisson's ratio, and shear moduli) of hybrids and (2) to determine the applicability of the available failgure criteria for combined-stress states in hybrids. Judiciously selected data for off-axis hybrids need to be generated.

Angleplied hybrids. - A large amount of data for angleplied hybrids (hybrid composite laminates made of alternating plies oriented at plus and minus angles to the load direction) has been generated and reported. The reason for this large amount of data is that many of the angleplied hybrids have been made to simulate composite components for specific applications.

Stress-strain diagrams for some typical angleplied hybrids are shown in figures 14 to 16[8] and figure 17[9]. The corresponding Poisson's strains are also shown in these figures. In figures 14 to 17, the stress-strain curves are approximately linear to fracture. This observation leads to the important conclusion that linear laminate theory should be applicable to angleplied hybrids.

Restrained strains in angleplied hybrids. - Thermally induced, restrained strains are present in angleplied hybrids as a result of differences between the use temperature and the lamination temperature. Restrained strains have been measured in some angleplied interply hybrids by the embedded strain gage technique. Some typical results of ply restrained strains are shown in figures 18 to 20[10].

The important points to be observed in figures 18 to 20 are (1) that the restrained strains are approximately linear in the temperature range 70° to 340° F and (2) that the transverse restrained strains (ε_{90}) are of considerably higher magnitude than the other restrained strains.

Lamination residual strains are equal in magnitude to restrained strains but of opposite sign. Therefore, the curves in figures 18 to 20 can be used to determine the lamination residual strains in the angleplied hybrids shown in these figures. For example, referring to figure 18, the transverse lamination residual strain (ε_{90}) in the Kevlar 49 plies of the $(0° \text{ Kev}/\pm 45° \text{ Gr}/0° \text{ Gr})_s$ composite is about 9000 µin./in. (opposite sign of -9×10^3). This is a very large strain when compared with the transverse tensile fracture strain of Kevlar 49, about 5000 µin./in. The important conclusion from this discussion is that transverse lamination residual strains in angleplied interply hybrids may be greater than the fracture strain of the constituent plies.

Stress Analysis of Hybrids

Stress analysis methods that have been used for hybrids are summarized with respect to composite mechanics, stress concentrations, fracture mechanics, and fatigue.

Composite mechanics. - Composite mechanics has been the principal stress analysis tool for hybrids. By far the majority of the hybrid analyses reported employ linear laminate theory (LLT)[2,6,7,11-13]. Laminate theory has been used in one of two ways: (1) to predict section properties for structural analysis and (2) to predict ply stresses having given the resultant forces at the section.

The influence of the constituent plies on the section properties and thermal forces of the hybrid is best illustrated by briefly examining the general LLT equations for determining these properties:

$$[A],[C],[D] = \sum_{i=1}^{N_\ell} \left[\int_{Z_{i-1}}^{Z_i} (1,Z,Z^2)[R]^T[E]^{-1}[R] \, dz \right]_i \tag{1}$$

$$\{N_T\},\{M_T\} = \sum_{i=1}^{N_\ell} \left[\int_{Z_{i-1}}^{Z_i} (1,Z)\ \Delta T\ [R]_i^T [E]^{-1} \{\alpha\}\ dZ \right]_i \qquad (2)$$

The notation in equations (1) and (2) is as follows: [A], [C], and [D] denote membrane, coupling and flexural (bending) stiffness matrices, respectively; these matrices are [3 × 3] for plane problems and [5 × 5] in cases where the transverse (through the thickness) shear deformations are taken into account. The term Z denotes the laminate thickness coordinate referred to some convenient plane; the index i denotes the ith ply in the stacking sequence of the laminate; $[R]_i$ denotes the transformation matrix locating the ith ply material axes (parallel to and transverse to the fiber direction) from the laminate structural axes (coincident with the principal load direction); $[E]_i$ denotes the ith ply stress-strain relations; $\{N_T\}$ and $\{M_T\}$ denote the thermal forces; ΔT_i denotes the difference between ply and reference temperature; and $\{\alpha\}_i$ denotes the ply thermal expansion coefficients. For extensive discussions on the application of equations (1) and (2) to composites and their limitations and use, see references 14 to 16.

Referring to equation (1), it is seen that the constituent plies influence the hybrid section properties (1) through the ply stress-strain relations $[E]_i$, (2) the ply orientation relative to the hybrid structural axes $[R]_i$, and (3) the ply location in the stacking sequence Z_i. Laminate configuration concepts such as the core/shell hybrid and the super-hybrid are readily deduced from equation (1). The ply properties used in equation (1) for interply hybrids are obtained either by measurement (table 1) or by the use of micromechanics. The ply properties for intraply hybrids are obtained by measurement. Composite micromechanics concepts in predicting intraply hybrid stress-strain relations were not reported in the literature summarized in this review.

Application of equation (1) to hybrids is valid if the hybrids have linear, or reasonably linear, stress-strain curves to fracture and if they have in situ ply stress-strain relations that are identical with those measured in characterizing the ply material. It will be recalled from the

previous section that resin matrix hybrids and superhybrids satisfy the first criterion; the second criterion may not always be satisfied. For example, predicted properties that are not coincident with the major fiber direction are not in good agreement with measured data[17].

Applying equation (2) to hybrids depends on whether the hybrid stress-strain-temperature relations are approximately linear in the temperature range of interest. The temperature effects on these relations for some interply hybrids were investigated[2]. The results showed that these relations are linear in the -65° to 250° F temperature range, with some degradation in the 250° to 350° F temperature range. We have also seen (figs. 18 to 20) that the thermally induced restrained strains are approximately linear in the same temperature range. It may be concluded from this discussion that LLT appears to be adequate for predicting section properties and thermal forces in hybrids.

Application of nonlinear laminate analysis to hybrids has not been reported in the literature summarized in this review. We expect that available nonlinear laminate analysis will be applicable to hybrids, provided that the appropriate ply stress-strain-temperature relations are used.

The LLT equation that has been used to predict ply strains in hybrids may be expressed in matrix form as follows:

$$\{\varepsilon\}_i = [R]_i \left\{ \left([A]^{-1} - z_i [C]_i^{-1} \right) \left(\{N_C\} + \{N_T\} \right) \right.$$

$$\left. + \left([C]_i^{-1} - z_i [D]_i^{-1} \right) \left(\{M_C\} + \{M_T\} \right) \right\} \tag{3}$$

where $\{\varepsilon\}_i$ denotes the strains in the ith ply; $\{N_C\}$ and $\{M_C\}$ denote resultant mechanical load forces and moments at the section; and $\{N_T\}$ and $\{M_T\}$ denote the corresponding thermal forces and moments. The other symbols have been defined previously.

The equation to predict ply stress in hybrids is obtained by multiplying equation (3) with the ply stress-strain relations and accounting for the free thermal strains. The resulting matrix equation may be expressed as follows:

$$\{\sigma\}_i = [E]_i \left(\{\varepsilon\}_i - \Delta T_i \{\alpha\}_i\right) \tag{4}$$

where $\{\sigma\}_i$ denotes the stresses in the ith ply of the hybrid; $\{\varepsilon\}_i$ is determined from equation (3); and the other symbols have been defined previously.

The strain predicted by equation (3) may be used in conjunction with the first ply-strain failure criterion to predict hybrid initial, or final, damage. Similarly, the stresses predicted by equation (4) may be used in conjunction with the first ply-stress failure criterion. In general, however, the stresses predicted by equation (4) have been used in conjunction with combined-stress failure criteria to predict hybrid failure, as is discussed later.

Experimental and predicted results for hybrid moduli and fracture stresses based on the maximum strain fracture criterion are compared in table 3[12,18]. The experimental data used in Kulkani[12] were obtained from Hoggatt[2]. The predicted values for the moduli for the hybrids in table 3 are in fair agreement with the experimental data. However, in the case of superhybrids[6] the predicted values for normal and flexural moduli and the Poisson's ratios (longitudinal and transverse) agree very well with the experimental data. As shown in table 3, the comparison for fracture stresses is poor. This may be attributed in part to differences in situ ply properties as compared with those used in the computations.

The maximum strain criterion in conjunction with LLT has been used by McKague[19] to generate interaction diagrams (failure envelopes) for a variety of hypothetical interply hybrids. A typical diagram is shown in figure 21[19]. The approach used by McKague[19] has been used extensively in designing composite structural components.

Combined-stress failure criteria. - Several combined-stress failure criteria have been proposed for composites[20,21]. The most commonly used is the von Mises-Hill criterion. In equation form, using the present notation, this criterion is[2]:

$$\left(\frac{\sigma_{1\alpha}}{S_{1\alpha}}\right)^2 + \left(\frac{\sigma_{2\beta}}{S_{2\beta}}\right)^2 - \left(\frac{\sigma_{1\alpha}\sigma_{2\beta}}{S_{1\alpha}S_{2\beta}}\right) + \left(\frac{\sigma_{12}}{S_{12}}\right)^2 = 1 \tag{5}$$

where σ denotes ply stress predicted from equation (4); S denotes the corresponding fracture stress measured under uniaxial loading; the numerical subscripts denote direction with 1 taken along the fiber direction; and the subscripts α and β denote tension and compression, respectively.

Equation (5) was used in reference 2 for comparisons with the experimental data. Some typical comparison results for the hybrids described in table 4[2] are shown in table 5[2]. Shown also in table 5 are values predicted by equation (5) when the ply fracture stresses S_{2T} and S_{12} are arbitrarily increased, as is indicated in footnote (c and d) to this table. Ply fracture stress was increased to account for possible differences in the in situ ply fracture stresses. In addition, the fracture stresses predicted by using the maximum stress (with and without increases in S_{2T} and S_{12}) and the maximum strain criteria are shown in the last three columns of table 5.

The predicted values (with and without in situ ply strength modifications) shown in table 5 agree poorly with the data. The correlation was improved for the compression data when specimens that were suspected to have failed by Euler buckling were excluded[2]. The conclusion, therefore, is that composite strength theories do not appear to be adequate for predicting the tensile fracture stress in hybrids.

Rule of mixtures. - The rule of mixtures (ROM) has been used to predict in-plane mechanical properties of interply unidirectional hybrids from constituent ply properties[5,7,22-24]. Reasonable agreement between predicted and experimental results were reported by Kalnin[7] for several in-plane properties, including transverse tensile strength.

Predicted and experimental results for longitudinal tensile fracture stress are compared in figure 22[24] for several interply Kevlar/graphite hybrids. Note the rapid initial drop (at low graphite fiber volume ratio) followed by a linear increase; this is consistent with what was described previously. Beyond the initial drop the predicted results agree well with the measured data.

The ROM has also been used to predict flexural properties of interply unidirectional hybrids[5,7]. Reasonable agreement with measured data was found when the moduli of the constituent plies were weighted according to

the ply's location in the stacking sequence as shown in the following
equation:

$$[E_{HF}] = \frac{1}{3t_H} \sum_i (z_{i+1}^3 - z_i^3)[E_i] \tag{6}$$

where E_{HF} denotes the flexural modulus of the hybrid; t_H denotes the
hybrid's thickness; Z_i is the distance from the reference plane to the
bottom of the ith ply; and Z_{i+1} is the distance from the reference plane
to the top of the ith ply.

From the foregoing, it appears that the RCM predicts mechanical proper-
ties of interply unidirectional hybrids that are in reasonable agreement with
experimental data. However, no unified and integrated theory especially
derived for hybrids has been reported in the literature summarized in this
review.

Stress concentrations in hybrids. - The analytical methods for determin-
ing stress concentrations in hybrids are the same as those used in conven-
tional composites. Usually, these methods include orthotropic or anisotropic
plate theory, and general or special-purpose finite-element analytical
methods. Results obtained from such analyses are subsequently compared with
measured data either at the ply level through LLT or at the hybrid level.
It was found by Fogg[25] that LLT underestimates the strength of hybrids with
holes because of the nonlinearities present in the hole vicinity. Inter-
laminar stresses near the free surfaces of holes and discontinuities may be
treated by using finite-element and finite-difference methods[26].

Fracture mechanics of hybrids. - The methods of analysis used are
directed toward determining the stress state at the crack tip and its imme-
diate vicinity. In this sense, orthotropic and anisotropic elasticity
theories are used, as well as special and general-purpose finite-element
methods. A recent symposium[27] examined the aspects of fracture mechanics
in composites in considerable depth. A current controversy in the field
focuses on the difficulty in defining what material properties govern un-
stable crack growth caused by the multitude of possible failure modes in
fiber composites.

It appears that linear elastic fracture mechanics (LEFF) concepts of metals may not be applicable to composites. The determination of fracture toughness properties of hybrids based on one configuration is not directly generalized to other configurations. It would seem, then, that more basic material properties probably govern the unstable crack growth.

One advantage of the hybrid concept mentioned previously is its inherent notch insensitivity or the existence of crack-arresting mechanisms that are derivable from the differences in stiffness and fracture strains of the different fibers used in the hybrid. An approximate method has been proposed to determine the size, spacing, and material of crack-arresting strips[28]. An application of this approach to large components is described by Huang[29].

Fatigue in hybrids. - An analytical method for predicting fatigue in interply unidirectional hybrids based on ROM concepts is described by Skudru[22]. However, as is the case for conventional composites, description of fatigue in hybrid laminates is empirical.

Structural Analysis of Hybrids

The structural analysis methods that have been used in hybrids are summarized with respect to classical methods and finite-element methods.

Classical methods. - All classical methods of analyzing the structures of composites[30-32] are applicable to hybrids, provided that the force deformation relations are appropriately modified.

The torsional and bending stiffness requirements in hybrid circular shafts (golf club shafts) were investigated by using slender-shaft structural analysis concepts[11]. The stability of hybrid composite columns and plates was investigated by using Euler buckling theory and classical plate-buckling theory, respectively[33]. The strength and stability of hybrid composite sandwich beams, plates, and shells were investigated by using structural sandwich theory[12].

Finite-element methods. - Finite-element methods that have been used in analyzing conventional composite components[34] are suitable for analyzing hybrid composite components as well. The appropriate force deformation relations are required, as was the case for the classical methods. Practically all major composite components include some form of hybrid. This may be

interply hybrid (or intraply) throughout the component, crack arresters, and/or local reinforcement for openings. In the majority of these cases, finite-element analytical methods are used to determine the structural response of the components[29,35].

Summary

The literature review of analytical methods led to the following observations:

1. Large amounts of data have been generated on the mechanical behavior of hybrids. In general, these data appear to be linear. Data for transverse compression, off-axis, and combined stress have not been reported.

2. Composite mechanics (LLT) appears to be adequate in predicting stiffness of hybrids in the linear range. Reasonable fracture stress correlation has been obtained in interply unidirectional composites. The correlation for angleplied hybrids is poor. A unified and integrated theory especially derived for hybrid composites appears to be needed.

3. Failure modes in hybrids under combined stress need to be quantified. Fracture stress predictions under combined stress using available criteria are inadequate and in situ ply properties need be quantified.

4. Structural analysis methods used in composite components appear to be adequate for hybrids, provided the force deformation relations have been appropriately modified.

DESIGN METHODS

The methods that have been used in the design of hybrid composite components are the same as those used for conventional composites. Design methods for composites in flight structures, including hybrids, have been the subject of three recent specialty conferences[36-38]. Composite design methods, in general, and examples for basic structural components are described by Chamis[39]. The review in this section is limited to pertinent design data of hybrids, some special design requirements that hybrids may satisfy effectively, and a summary of specific designs where advantage has been taken of one or more of the special features of hybrid composites.

Design Data for Hybrid Composites

Design data usually consist of mechanical and thermal material proper-
ties and environmental effects on these properties. Typical mechanical
properties data for hybrids have been discussed in previous sections. Avail-
able data for environmental effects on these properties are reviewed herein.
The environmental effects include temperature, moisture, mechanical load
fatigue, thermal fatigue, and thermal shock. Also, limited data on the re-
sistance of hybrids to high-velocity impact are included.

The effects of temperature for short-time exposures on the mechanical
properties of hybrid composites were reported by Hoggatt[2] and are shown in
figures 23 to 27. Curves are shown for three different load directions 0°,
45°, and 90°. The 0° direction coincides with the largest number of 0°
plies. The temperature effects on the tensile fracture stress are shown in
figure 23 for the temperature range -65° to 350° F. Two important points to
be observed from figure 23 are

1. The temperature effects on the tensile fracture stress are negligible
in the 0° to 250° F range for all three load directions.

2. A small degradation in tensile fracture stress occurs from 0° to
-65° F and from 250° to 350° F.

The effects of temperature on the compressive fracture stress of hybrids
are shown in figure 24. The compressive fracture stress is sensitive to
temperatures, in general, from room temperature to 350° F.

The effects of temperature on tensile modulus are shown in figure 25.
The temperature effects on the tensile modulus in the 0° ply direction are
negligible. Some degradation occurs in the other two load directions in the
room-temperature to 350° F range. An increase in modulus occurs in the 90°
ply direction in the room-temperature to -65° F range.

The temperature effects on the Poisson's ratio of hybrids are shown in
figure 26. Poisson's ratio appear to be sensitive to temperature and, also,
to load direction at temperature.

The temperature effects on the in-plane (intralaminar) shear fracture
stress and shear modulus of hybrids are shown in figure 27. These properties
exhibit erratic behavior with decrease or increase in temperature. The

thermal expansion coefficients (TEC), as shown in table 6, are not affected by changes in temperature in the $-100°$ to $300°$ F range[2].

The effects of moisture on the flexural strength and flexural modulus of a hybrid are shown in figure 28[2]. The presence of moisture increases the room-temperature properties but produces a small reduction in the $350°$ F fracture stress. Though data are not available in the review summarized herein, it is generally known that the fracture modes may change with increases in temperature, moisture, or both.

Fatigue strength data of hybrids have been reported in references 2, 4, and 8. Selected fatigue data on interply unidirectional hybrids and their constituents are shown in figure 29[4]. The fatigue data for the hybrid lie between its two constituents. It can be seen in figure 29 that the fatigue life of the S-glass (S-GL) composite decreases nonlinearly with the log of the number of cycles to failure in the range shown, while the fatigue lives of Modmor II and all the hybrids plotted decrease linearly. These observations appear to lend some support to the use of the rule of mixtures to predict the fatigue life of unidirectional hybrids by using the fatigue lives of the constituents[22].

Selected fatigue data of angleplied interply hybrids and their constituents are shown in figure 30[8]. The fatigue lives of the hybrids lie between those of the constituents, as was the case for the unidirectional hybrids.

The temperature of the hybrid specimen rises during fatigue testing. This rise depends on the constituent composites and the cyclic load frequency. Temperature increases of $130°$ F have been measured. This temperature increase may change the fracture mode and, therefore, should be an important consideration in studying fatigue fracture modes.

Thermal fatigue (500 cycles, $-65°$ to $300°$ F over a 30-min period) has negligible effect on the tensile fatigue life of hybrids[2]. Interlaminar-shear thermal fatigue data are shown in figure 31[2], and the effect is negligible. Thermal fatigue (1000 cycles, $-100°$ to $300°$ F) has negligible effect on the room-temperature longitudinal and transverse flexural strength of superhybrids[40].

Thermal shock (100 cycles, -65° to 300° F by immediate immersion) has no effect on the room-temperature tensile strength and tensile modulus of angleplied interply hybrids[2]. However, some hybrids containing S-GL delaminated during thermal shock cycling. Some delamination also occurred during thermal fatigue of angleplied hybrids with S-GL constituents[2].

The impact resistance of hybrid composites has been investigated extensively. Hybridization with high-strength fibers considerably improves the impact resistance of relatively brittle composites[5,13,24,41-43]. The data in these references are useful in designing for impact resistance; selected samples are included herein. Izod impact resistance of graphite/Kevlar hybrids improved with increased content of Kevlar fibers (fig. 32[24]). The addition of 20-vol% Kevlar almost doubled the impact resistance of the HMS graphite composites.

Data that may be useful in trading off between flexural modulus and impact resistance are shown in figure 33[5]. The approximate lower bound required on the flexural modulus (19×10^6 psi) is shown by the dashed line in figure 33. This bound was selected to satisfy vibration requirements in laminate configurations for engine fan blade applications. As shown, a design condition requiring a flexural modulus of 19 msi and an impact resistance of 120 ft-lb/in.[2] or greater can only be satisfied by hybridization. The impact resistance of some superhybrids is shown in table 7[40]. The impact resistances of B/Al composites are also shown for comparison. The longitudinal impact resistance of superhybrids is shown to be about twice that of B/Al.

Special Design Requirements

It was mentioned previously that hybrids have been developed to meet diverse competing design requirements. An example of these competing requirements is the high flexural modulus and high impact resistance illustrated in figure 33. Another example is flexural modulus and cost, illustrated in figure 34[5], which indicates that a high flexural modulus can be achieved at lower cost by hybridization.

These examples are from parametric and/or trade-off studies. Data from a large number of hybrids that can be used for these studies are

available[12]. A more direct approach for a specific design is automated design and optimization by mathematical programming. This approach was used to identify hybrids for optimum cost[2] and to design structural components such as sandwich beams, plates, and shells for minimum cost or minimum weight[12]. Examples of specific designs may be found in the section APPLICATION OF HYBRID COMPOSITES.

Summary of Specific Designs using Hybrid Composites

The special features of hybrids have been used advantageously in the following designs: mechanical fatigue improvement of helicopter rotor blades[44]; survivability of helicopter rotor blades when subjected to large-caliber ground fire; damage tolerance in fuselage-like structures[29]; damage tolerance by means of softening strip in spar caps[25]; minimization of wing-box-face waviness, which had caused premature failures[45]; stiffness improvement in stiffness-critical designs of thin tubes[11]; stiffness improvement and damage tolerance in vertical stabilizers and in horizontal stabilizers; and impact improvement in compressor blades[46-48].

APPLICATION OF HYBRID COMPOSITES

Specific applications of hybrid composites reported in the literature reviewed were as follows: a 10-foot-long outboard section of a helicopter rotor[2]; helicopter rotors; aircraft components such as upper and lower wing surfaces, shear web, and fuselage upper crown[44]; fuselage component (25-in. diam by 41 in. long)[29]; upper and lower skins of the outer wing section for A70 aircraft[35]; sporting goods such as golf club shafts, bicycle frames, and tennis racquets[49]; box beam[45]; inboard aileron of the L-1011 aircraft[25]; aircraft fuselage panels, bows, golf shafts[24]; space shuttle thrust truss support[50]; vertical stabilizer for the B-1; compressor fan blades for aircraft engines[46-48]; theoretical studies for helicopter aft fuselage tail boom; and a horizontal stabilizer[51].

Two hybrid composite compressor blades are shown in figure 35 (interply) and figure 36 (intraply)[46]. As can be deduced from this list, the application of hybrid composites has been mainly in the aircraft and sporting industries.

FABRICATION PROCEDURES FOR HYBRID COMPOSITES

The fabrication procedures used for hybrid composites are the same as those used for conventional composites. A comprehensive review of the fabrication methods for composites is compiled in **reference 3. Additional** emphasis is placed on low-cost fabrication procedures and field **repairs**[44]. Some typical fabrication costs are summarized in **table** 8^2.

The cocuring process may be unique to hybrids since each composite within the hybrid has been optimized with respect to a fiber/matrix combination. The cocuring process for hybrids has been **investigated**[2] and the optimum cure cycle was shown to be a compromise between the cure cycles of the individual composites. Typical mechanical properties data from this cocuring study are summarized in table 9^2. The cocuring process appears to improve the mechanical properties. A variety of fabrication procedures including the use of polyimides and PPQ (**polyphenylquinoxaline**) resins for making **interply** and **intraply** hybrids are described by **Pike**[5].

Fabrication procedures for specific hybrids are described in the literature reviewed as follows: Kevlar/graphite hybrids[2,4,5,8,9,24,42]; S-glass or E-glass/graphite hybrids[2,4,5,8,9,42]; boron/graphite hybrids[2]; boron/S-glass hybrids[2]; boron/glass/graphite/Kevlar hybrids[46,47]; thermoplastic resins[52,53]; superhybrids[6,40,53].

Nondestructive evaluation methods (NDE) and inspection techniques that have been used in quality assurance for conventional composites are applicable to hybrid composites as well. Assuring the quality of components made from hybrid composites was not identified as a special problem for hybrids in the literature reviewed and summarized herein.

From our literature review, we conclude that fabrication procedures for the various hybrids are well in hand.

AREAS FOR FURTHER RESEARCH

Based on the data reviewed, the following areas (not prioritized) need further research:

1. Experimental

   a. Evaluation of the transverse compression properties of interply unidirectional hybrids

    b. Complete characterization of intraply hybrids

    c. Evaluation of off-axes properties of hybrids

    d. Evaluation of combined-stress fracture in hybrids

    e. Identification and quantification of fracture modes in hybrids

    f. Assessment of in situ ply properties relative to unidirectional material

    g. Additional fatigue data - compression stress reversal and shear

    h. Effects of temperature and/or moisture on fatigue life

    i. Evaluation of thermal properties - thermal coefficients of expansion, heat conductivity, heat capacity

    j. Design data generated from generally accepted test methods

2. Theoretical

    a. Composite mechanics for intraply hybrids

    b. Nonlinear laminate theory for hybrids

    c. Strength theory for angleplied interply and intraply hybrids

    d. Unified and integrated theory for hybrid composites

    e. Theoretical description of fatigue of hybrids

    f. Life prediction in controlled and service environments

CONCLUDING REMARKS

The significant findings and conclusions from a state-of-the-art review on the analysis, design, application, and fabrication of hybrid composites are as follows:

1. Considerable data have been generated for the tensile strength properties, as well as the tensile and thermal fatigue, of interply hybrids.

2. Limited data have been generated on the thermal properties, moisture effects, and effects of residual strains in interply hybrids.

3. Considerable data have been generated for impact resistance of interply and intraply hybrids.

4. The rule of mixtures appears to be adequate for predicting longitudinal and transverse mechanical properties of unidirectional interply hybrids.

5. Linear laminate theory appears to be adequate for predicting the elastic response of hybrids.

6. Stress and structural analysis methods, design procedures, fabrication methods, and quality assurance techniques that are used for conventional composites are also suitable for hybrids.

7. Structural components can be designed to meet diverse and competing design requirements.

8. Areas that need further research are complete characterization of intraply hybrids, off-axes and combined stresses, compressive and reverse fatigue, quantification of fracture modes and in situ ply properties, temperature and moisture effects, thermal properties, strength prediction theory, nonlinear laminate theory for hybrids, theoretical description of fatigue, and development of a unified and integrated theory for hybrid composites.

REFERENCES

1. Chamis, C. C., Hanson, M. P., and Serafini, T. T., "Criteria for Selecting Resin Matrices for Improved Composite Strength," Proceedings of the Twenty-Eighth Annual Conference on Reinforced Plastics - Ever New, Society of the Plastics Industry, Inc., 1973, pp. 12-C, 1 to 12-C, 12.

2. Hoggatt, J. T., and R. G. Cheatham. "Evaluation of Hybrid Composites." June 1974-Oct. 1975, Boeing Aerospace Co.

3. "Structural Design Guide for Advanced Composite Applications," 3rd ed., Lab., Wright-Patterson AFB, Ohio, 1973.

4. Rao, Nagaraja, and Hofer, K. E., Jr., "Fatigue Behavior of Graphite/ Glass/Epoxy Composites," Proceedings of the International Conference on Carbon Fibers, Their Place in Modern Technology, Plastics Institute, 1974.

5. Pike, R. A., and Novak, R. C., "Design, Fabrication and Test of Multi-Fiber Laminates," R75-911730-15, Jan. 1975, United Aircraft Corporation; also NASA CR-134763.

6. Chamis, C. C., Lark, R. F., and Sullivan, T. L., "Boron/Aluminum-Graphite/Resin Advanced Fiber Composite Hybrids," NASA TN D-7879, 1975.

7. Kalnin, I. L., "Evaluation of Unidirectional Glass - Graphite Fiber/ Epoxy Resin Composites," Proceedings of the Second Conference on Composite Materials. Testing & Design, STR 497, American Society for Testing and Materials, 1972, pp. 551-563.

8. Liber, T., and Daniel, I. M., "Evaluation of Hybrid Composite Materials in Cylindrical Specimen Geometries," IITRI-D6089, Mar. 1976, IIT Research Institute; also NASA CR-145006.

9. Daniel, I. M., and Liber, T., "Lamination Residual Strains and Stresses in Hybrid Laminates," presented at the ASTM Fourth Conference on Composite Materials; Testing and Design, Valley Forge, Pa., May 3-4, 1976.

10. Daniel, I. M., and Liber, T., "Lamination Residual Stresses in Hybrid Composites." Part I. (Illinois Inst. Tech., NAS3-16766) CR-135085, 1976, NASA.

11. Kliger, H. S., "Ultra-High-Modulus Graphite Hybrids for Combined Torsion and Extensional Rigidity," 31st Annual SPI Conference, Society of the Plastics Industry, Inc., 1976, Paper 12A.

12. Kulkarni, S. V., Rosen, B. W., and Boehm, H. C., "Evaluation of Hybrid Composite Materials." MSC/TFR/507, June 1975, Materials Science Corporation (AFML-TR-75-92; AD-A021688).

13. Chamis, C. C., Hanson, M. P., and Serafini, T. T., "Design for Impact Resistance with Unidirectional Fiber Composites," NASA TN D-6463, 1971.

14. Ashton, J. E., Halpin, J. C., and Pellit, P. H., "Primer on Composite Materials: Analysis," 1969, Technomic.

15. Sendeckyj, G. P., ed., Mechanics of Composite Materials, Academic Press, 1974.

16. Jones, R. M., Mechanics of Composite Materials, McGraw-Hill, 1975.

17. Chamis, C. C., and Sullivan, T. L., "Combined-Load Stress-Strain Relationships for Advanced Fiber Composites," NASA TMX-71825, 1976.

18. Kulkarni, S. V., Rosen, B. W., and Boehm, H. C., "Cost-Performance Evaluation of Hybrid Composite Materials." _Proceedings of the 31st Annual SPI conference, Society of_ the Plastics Industry, Inc., 1976, Paper 17A.

19. McKague, E. L., Jr., "Hybrid Laminate Analysis," ERR-FW-1398, Dec. 1972, General Dynamics.

20. Wu, E. M., "Phenomenological Anisotropic Failure Criterion," _Composite Materials. Volume 2: Mechanics of Composite Materials_, G. P. Sendeckyj, ed., Academic Press, 1974, pp. 353-431.

21. Vicario, A. A., Jr., and Toland, R. H., "Failure Criteria and Failure Analysis of Composite Structural Components," _Composite Materials. Volume 7: Structural Design and Analysis, Part I_, C. C. Chamis, ed., Academic Press, 1975, pp. 51-97.

22. Skudra, A. M., et al., "Properties of Fiberglass-Plastics Reinforced with High-Modulus Fibers." _Mechika Polimerov_, Jan.-Feb. 1972, pp. 68-74.

23. Bunsell, A. R., and Harris, B., "Hybrid Carbon and Glass Fibre Composites," _Composites_, Vol. 5, June 1974, pp. 157-164.

24. Reewald, P. G., and Zweeben. C., "Kevlar 49 Hybrid Composites for Commercial and Aerospace Applications." _Proceedings of the 30th Annual SPI Conference_, Society of the Plastics Industry, Inc., 1975, Paper 14B.

25. Private communication on hybrid composite design for damage tolerance from L. D. Fogg of Lockheed Aircraft Co., Burbank, Calif.

26. Grimes, G. C., and Greimann, L. F., "Analysis of Discontinuities, Edge Effects, and Joints," _Composite Materials. Volume 8: Structural Design and Analysis, Part II_, C. C. Chamis, ed., Academic Press, 1976, pp. 135-230.

27. _Fracture Mechanics of Composites_, STP 593, American Society for Testing and Materials, 1975.

28. Sendeckyj, G. P., "Concepts for Crack Arrestment in Composites," Fracture Mechanics of Composites, STP-593, American Society for Testing and Materials, 1975, pp. 215-226.

29. Huang, S. L., and Hess, T. E., "A Hybrid Composite Fuselage Design with Integral Crack Arresters." Third Conference on Fibrous Composites in Flight Vehicle Design, NASA TM X-3377-Pt-2, 1976, pp. 737-758.

30. Knoell, A. C., and Robinson, E. Y., "Analysis Truss, Beam, Frame, and Membrane Components," Composite Materials. Volume 7: Structural Design and Analysis, Part I, C. C. Chamis, ed., Academic Press, 1975, pp. 99-148.

31. Bert, C. W., "Analysis of Plates," Composite Materials. Volume 7: Structural Design and Analysis, Part I, C. C. Chamis, ed., Academic Press, 1975, pp. 149-206.

32. Bert, C. W., "Analysis of Shells," Composite Materials. Volume 7: Structural Design and Analysis, Part I, C. C. Chamis, ed., Academic Press, 1975, pp. 207-258.

33. Berg, K. R., "Graphite Reinforcing of Glass Composite Structures," Proceedings of the 27th Annual SPI Conference, Society of the Plastics Industry, Inc., 1972, pp. 17-E,1 to 17-E,4.

34. Purdy, D. M., "Discrete Element Analysis of Composite Structures," Composite Materials. Volume 8: Structural Design and Analysis, Part I, C. C. Chamis, ed., Academic Press, 1975, pp. 1-31.

35. Foreman, C. R., and Tanis, C., "Development of an A-7D Advanced Composite Outer Wing for Production and In-Service Experience," Third Conference on Fibrous Composites in Flight Vehicle Design, NASA TM X-3377-Pt-1, 1976, pp. 143-164.

36. Proceedings of the Conference on Fibrous Composites in Flight Vehicle Design, AFFDL-TR-72-130, Dec. 1972, Wright-Patterson AFB.

37. Proceedings of the Second Conference on Fibrous Composites in Flight Vehicle Design, AFFDL-TR-74-103, Sept. 1974, Wright-Patterson AFB.

38. "Third Conference on Fibrous Composites in Flight Vehicle Design," NASA TM X-3377, pts. 1 and 2, 1976.

39. Chamis, C. C., "Design of Composite Structural Components," _Composite Materials._ _Volume 8:_ _Structural Design and Analysis, Part I_, C. C. Chamis, ed., Academic Press, 1975, pp. 231-280.

40. Chamis, C. C., Lark, R. F., and Sullivan, T. L., "Super-Hybrid Composites - An Emerging Structural Material." Third Conference on Fibrous Composites in Flight Vehicle Design, NASA TM X-3377-Pt. 2, 1976, pp. 851-877.

41. Novak, R. C., and Decrescente, M. A., "Impact Behavior of Unidirectional Resin Matrix Composites Tested in the Fiber Direction," _Proceedings_ _of the Second Conference on Composite Materials; Testing and Design_, STP-497, American Society for Testing and Material, 1972, pp. 311-323.

42. Friedrich, L. A., and Preston, L. J., "Impact Resistance of Fiber Composite Blades Used in Aircraft Turbine Engines," PWA-4727, May 1973, Pratt & Whitney Aircraft; also NASA CR-134502.

43. Simon, R. A., "Impact Strength of Carbon Fiber Composites." _Proceedings_ _of the Twenty-Eighth Annual Conference on Reinforced Plastics._ _Ever_ _New_, Society of the Plastics Industry, Inc., 1973, pp. 17-B,1 to 17-B,8.

44. Salkind, M. J., "New Composite Helicopter Rotor Concepts," _Proceeding_ _of the Conference of Fibrous Composites in Flight Vehicle Design_, AFFDL-TR-72-130, Dec. 1972, Wright-Patterson AFB, p. 57.

45. Hadcock, R. N., et al., "Design and Fabrication of a Mixed Composite Wing Box," _presented at SAMPE 5th National Symposium_, October 9-11, 1973.

46. "Impact Resistance of Composite Fan Blades," R74AEG320, Dec 1974, General Electric Co.; also NASA CR-134707.

47. Oller, T. L., "Fiber Composite Fan Blade Impact Improvement Program." (General Electric; NAS3-17836), NASA CR-135078, 1976.

48. "Low Cost FOD Resistant Organic Matrix Fan Blades." Contract F-33615-74-C-5072, AFML, Wright-Patterson AFB, Ohio, Final report, 1977.

49. Private communication on application of hybrids to sporting goods from P. R. Hoffman of Avco, Lowell, Mass., 1975.

50. Corvelli, N., and Carri, R., "Evaluation of Boron-Epoxy-Reinforced Titanium Tubular Truss for Application to a Space Shuttle Booster Thrust Structure," NASA TN D-6778, 1972.

51. Hadcock, R. H., "The Application of Mixed Fiber Composites to Military Aircraft," presented at the 10th National State-of-the-Art Symposium, American Chemical Society, June 10-12, 1974.

52. Long, W. G., "Reinforced Thermoplastics." Apr. 1974, Babcock and Wilcox Corporation (AD-782760; AMMRC-CTR-74-32; TRG-74-10).

53. Novak, R. C., "Multi-fiber Composites," R76-912098-11, Apr. 1976, United Technologies Research Center; also NASA CR-135062.

TABLE 1. - UNIDIRECTIONAL COMPOSITE PROPERTIES: TYPICAL ROOM TEMPERATURE VALUES[a]

Material	Epoxy matrix resin	Form	Fiber volume ratio	Density (g/cm³)	Density (lb/in³)	Longitudinal (0°) properties Tension Strength, ksi	Tension Modulus, msi	Compression Strength, ksi	Compression Modulus, msi	Transverse (90°) tension Strength, ksi	Modulus, msi	Flexural properties Strength, ksi	Modulus, msi	Interlaminar (short beam) shear strength, ksi	In-plane (intralaminar) shear properties Strength, ksi	Modulus, msi	Poisson's ratio	Ply thickness, mils	Prepreg cost, $/lb
Boron	5505	Tape	0.50	1.99	0.072	230	30	360	32	9.1	2.7	---	----	16.0	19.0	0.93	0.21	5.2	150
Graphite:																			
A-S	3501	Tape	0.60	1.54	0.055	210	18.5	170	16	9.0	1.3	225	17	14	8.7	0.83	0.25	5-8	45
PMS	934			1.63	.059	120	30	90	25	12.5	2.0	150	28	10.5	10.4	.85	.20	7-8	75
HTS	5208			1.55	.056	215	25	155	24	13	1.3	245	23	16.5	10.5	.85	.21	7-8	65
T-300	5208					210	20	210	20	6.5	1.5	260	20	14	9.0	.95	.21	5-7	45
GY-70	934			1.69	.061	85	40	75	38	6.0	1.2	135	38	7.5	14.0	.60	.25	6-8	60
MOD-I	5208			1.67	.060	120	31	100	29	12.0	2.0	186	29	10	10.4	.85	.22	6-8	75
MOD-II	5208			1.54	.050	186	24	100	23	9.7	1.9	210	23	14.9	15.8	.72	.38	6-8	65
Kevlar-49	-----	Tape	0.60	1.38	0.050	200	11.0	40	11	4.1	0.8	90	11	7.0	8.7	0.3	0.34	5-7	45
Kevlar-29	-----	Tape	.60	1.38	.050	200	5.0	40	5.0	4.1	.7	90	5.0	6.0	8.7	.3	.34	5-7	20
Nomex	-----	Tape	0.60	----	-----	---	----	---	----	-----	-----	---	----	----	----	-----	-----	---	55
Glass:																			
E	1002	Tape	0.60	1.80	0.065	160	5.7	90	4.6	[b]14	[b]0.7	165	5.3	10.0	12.0	[b]0.7	[b]0.3	10	2.35
901-S	1002S	Tape	.60	1.82	.066	215	6.3	120	6.0			200	6.0	11.2	12.0			10	17.60
S2-S	1002S	Tape	.60	1.82	.066	180	6.3	110	6.0			170	6.0	10.5	12.0			10	6.20

[a] From ref. 2.
[b] Average values.

TABLE 2. - INTERPLY HYBRID DESCRIPTION[a]

Laminate	Material	Configuration[b]
1	S-GL/T-300/S-GL	$(0^\circ_4/\pm45^\circ/90^\circ)_s$
2	T-300/B/T-300	$(0^\circ_4/\pm45^\circ/90^\circ)_s$
3	B/T-300/T-300	$(0^\circ_4/\pm45^\circ/90^\circ)_s$
4	S-GL/B/S-GL	$(0^\circ_4/\pm45^\circ/90^\circ)_s$
5	Kev 49/T-300/Kev 49	$(0^\circ_4/\pm45^\circ/90^\circ)_s$
6	T-300/HMS/T-300	$(0^\circ_4/\pm45^\circ/90^\circ)_s$
7	HTS/B/T-300	$(0^\circ_4/\pm45^\circ/90^\circ)_s$
8	S-GL/HMS/S-GL	$(0^\circ_4/\pm45^\circ/90^\circ)_s$
9	S-GL/G-181/S-GL	$(0^\circ_4/45^\circ/90^\circ)_s$
10	S-181/G-181	$(0^\circ_4/45^\circ)_s$
11	S-GL/Kev 49-328/S-GL	$(0^\circ_4/45^\circ/90^\circ)_s$
12	T-300/G-181	$(0^\circ_4/45^\circ/90^\circ)_s$
13	AS/Kev 49-181	$(0^\circ_4/45^\circ/90^\circ)_s$
14	G-248/G-181/G-248	$(0^\circ_2/45^\circ/90^\circ)_s$
15	HTS/G-181/HTS	$(0^\circ_4/45^\circ/90^\circ)_s$
16	Kev 49/G-181F/Kev 49	$(0^\circ_4/45^\circ/90^\circ)_s$

[a]From ref. 2.
[b]Subscripts following the numbers indicate
number of plies in that direction. The
subscript "s" following the parenthesis
denotes that laminate is symmetrical about
last ply in sequence.

TABLE 3. - COMPARISON OF EXPERIMENTAL DATA WITH THEORETICAL PREDICTION FOR SELECTED BOEING LAMINATES[a]

Material	Configuration	Tensile failure stress, ksi		Compressive failure stress, ksi		Modulus (longitudinal), msi			Modulus (transverse), msi		
		Test	Theory[b]	Test	Theory[b]	Test		Theory	Test		Theory
						Tension	Compression		Tension	Compression	
S-GL/T-300	$(0^\circ_4/\pm45^\circ_2)_s$	141.5	(31.0) 141.0	96.5	(31.0) 81.0	6.9	5.7	5.3	3.1	3.3	2.5
T-300/B	$(0^\circ_4/\pm45^\circ)_s$	157.5	167.2	98.7	(104.7) 157.0	21.4	17.0	15.9	4.4	2.6	3.2
B/T-300/T-300	$(0^\circ_3/\pm45^\circ/90^\circ)_s$	124.2	127.3	95.0	(182.3) 185.9	22.0	3.5	17.4	8.4	2.2	4.2
S-GL/B	$(0^\circ_5/\pm45^\circ)_s$	241.5	(81.5) 189.0	75.1	(78.3) 108.0	7.2	7.1	6.0	4.3	3.4	1.9
Kev 49/T-300/Kev 49	$(0^\circ_2/\pm45^\circ_2/90^\circ)_s$	72.0	(33.9)	25.5	29.8	7.0	5.7	6.0	4.0	3.0	3.9
T-300/HMS	$(0^\circ_4/\pm45^\circ_3)_s$	92.0	(97.0)	79.1	(56.2) 84.0	10.8	10.4	9.9	3.6	3.1	4.4
HTS/B	$(0^\circ_5/\pm45^\circ)_s$	116.0	160.2	90.7	211.9	10.8	12.8	17.2	3.6	2.5	3.1
S-GL/HMS	$(0^\circ_4/\pm45^\circ)_s$	109.0	(47.3) 114.0	57.9	(47.3) 65.0	2.8	5.3	4.8	1.1	2.7	3.0

[a] From ref. 12.
[b] Numbers in parentheses denote a matrix failure.

TABLE 4. - HYBRID COMPOSITES TESTED IN REFERENCE 2

Laminate $(0^\circ/\pm45^\circ/90^\circ)$	Material	Panel	Longitudinal (0°) tension, compression, and shear coupons
1	S-GL/T-300/S-GL	1	$(0^\circ_4/\pm45^\circ/90^\circ)_s$
		2	$(0^\circ/\pm45^\circ_2/90^\circ)_s$
		3	$(0^\circ_4/\pm45^\circ_2)_s$
2	T-300/B/T-300	1	$(0^\circ_4/\pm45^\circ/90^\circ)_s$
		2	$(0^\circ/\pm45^\circ_2/90^\circ)_s$
		3	$(0^\circ_4/\pm45^\circ)_s$
3	B/T-300/T-300	1	$(0^\circ_4/\pm45^\circ/90^\circ)_s$
		2	$(0^\circ/\pm45^\circ/90^\circ)_s$
		3	$(0^\circ_3/\pm45^\circ/90^\circ)_s$
4	S-GL/B/S-GL	1	$(0^\circ_4/\pm45^\circ/90^\circ)_s$
		2	$(0^\circ/\pm45^\circ/90^\circ)_s$
		3	$(0^\circ_5/\pm45^\circ)_s$
5	Kev 49/T-300/Kev 49	1	$(0^\circ_4/\pm45^\circ/90^\circ)_s$
		2	$(0^\circ/\pm45^\circ_2/90^\circ)_s$
		3	$(0^\circ_2/\pm45^\circ_2/90^\circ)_s$
6	T-300/HMS/T-300	1	$(0^\circ_4/\pm45^\circ/90^\circ)_s$
		2	$(0^\circ/\pm45^\circ_2/90^\circ)_s$
		3	$(0^\circ_4/\pm45^\circ_3)_s$
7	HTS/B/T-300	1	$(0^\circ_4/\pm45^\circ/90^\circ)_s$
		2	$(0^\circ/\pm45^\circ_2/90^\circ)_s$
		3	$(0^\circ_5/\pm45^\circ)_s$
8	S-GL/HMS/S-GL	1	$(0^\circ_4/\pm45^\circ/90^\circ)_s$
		2	$(0^\circ/\pm45^\circ_2/90^\circ)_s$
		3	$(0^\circ_4/\pm45^\circ_3)_s$

F-8980

TABLE 5. - COMPARISON OF MEASURED AND PREDUCTED TENSILE FRACTURE STRESSES OF HYBRIDS SHOWN IN TABLE 4[a]

Laminate	Material	Panel[b]	Fracture stress, average ksi	Predicted tensile fracture stresses, S_{XT}, ksi					
				Von Mises-Hill	Von Mises-Hill[c]	Von Mises-Hill[d]	Maximum stress	Maximum stress[c]	Maximum strain
1	S-GL/T-300/S-GL	1	122.4	32.9	48.4	137.8	39.4	59.1	20.9
		2	53.4	22.8	33.7	101.1	26.0	39.0	14.5
		3	141.5	29.7	44.4	150.5	31.1	46.6	117.5
2	T-300/B/T-300	1	128.4	63.3	92.7	140.7	64.7	97.0	68.1
		2	37.0	39.9	58.2	88.1	40.9	61.3	42.7
		3	157.5	141.4	147.2	147.2	155.5	**155.5**	**139.8**
3	B/T-300/T-300	1	95.6	89.1	132.7	151.6	89.5	134.3	98.9
		2	48.1	35.1	51.3	57.0	35.9	53.8	37.7
		3	124.2	147.5	177.7	177.7	172.5	180.8	152.6
4	S-GL/B/S-GL	1	133.2	43.7	62.8	116.6	58.4	87.2	21.1
		2	53.6	36.7	53.3	97.7	51.1	76.7	16.0
		3	241.5	56.3	81.9	149.4	74.5	111.8	131.1
5	Kev 49/T-300/Kev 49	1	116.2	49.3	58.6	71.0	60.4	77.5	63.6
		2	57.2	29.5	34.2	40.0	36.6	43.1	39.9
		3	72.0	36.9	41.4	46.2	47.1	49.2	54.1
6	T-300/HMS/T-300	1	105.0	60.8	89.2	135.8	62.0	93.0	65.5
		2	40.5	30.2	44.0	66.5	30.9	46.4	32.3
		3	92.0	72.4	104.9	104.9	75.3	112.4	101.0
7	HTS/B/T-300	1	77.0	69.7	101.9	132.9	71.2	106.9	74.8
		2	26.6	34.0	49.5	64.4	35.0	52.5	36.3
		3	116.5	165.2	165.2	165.2	169.4	169.4	160.0
8	S-GL/HMS/S-GL	1	117.8	36.3	49.6	80.4	43.0	64.5	20.8
		2	42.3	27.0	38.5	75.1	29.4	44.2	15.5
		3	109.6	28.6	42.1	107.7	29.3	44.0	71.9

[a]From ref. 2.
[b]Refers to hybrid configuration shown in table 4.
[c]S_{2T} and S_{12} are 1.5 times the values shown in table 1.
[d]S_{2T} and S_{12} = 50 ksi.

TABLE 6. – THERMAL EXPANSION MEASUREMENTS (-100° F TO +300° F)[a]

Material	Configuration	Thermal expansion coefficient, in./in./°F	
		Longitudinal (0°)	Transverse (90°)
Kev 49/T-300/Kev 49	$(0^o_4/\pm45^\circ/90^\circ)_s$	-0.76×10^{-6}	3.0×10^{-6}
T-300/HMS/T-300	$(0^o_4/\pm45^\circ/90^\circ)_s$	3.4	3.8
S-181/G-181	$(0^o_4/45^\circ)_s$	3.3	4.0
Kev 49/G-181F/Kev 49	$(0^o_4/45^\circ/90^\circ)_s$	-.64	3.1

[a]From ref. 2.

TABLE 7. – SUPERHYBRID THIN-SPECIMEN IZOD IMPACT STRENGTH[a]

Constituents	Test direction	Izod impact strength in-lb/in^2		Number of specimens
		Low	High	
B/Al (5.6-mil-diam fiber)[b]	Longitudinal	331	335	3
	Transverse	135	167	2
B/Al (8.0-mil-diam fiber)[b]	Longitudinal	319	338	3
	Transverse	129	147	2
Ti, B/Al,[c] Gr/Ep,[d] Ti	Longitudinal	634	720	2
	Transverse	186	202	2
Ti, Gr/Ep[c]	Longitudinal	573	734	3
	Transverse	142	171	3
Ti, B/Al,[c] Gr/Ep	Longitudinal	454	658	6
	Transverse	129	143	2

[a]From ref. 40.
[b]Diffusion-bonded, 1100 aluminum alloy.
[c]Adhesive bonded.
[d]Graphite/epoxy.

TABLE 8. – SUMMARY OF FABRICATION COSTS FOR

ALL HYBRIDS SHOWN IN TABLE 4[a]

Form	Method	Fabrication rate, lb/hr	Fabrication cost, $/lb
3-Inch tape	Hand layup	2.5 – 3.5	4.25 – 6.00
	Machine assist	5 – 6	2.50 – 3.00
	Automatic machine	4 – 5	3.00 – 3.75
12-Inch tape	Hand layup	4 – 5	3.00 – 3.75
	Machine assist	8 – 10	1.50 – 1.90
24-Inch fabric	Hand layup	7.5 – 8.5	1.75 – 2.00
36-Inch fabric	Hand layup	8 – 10	1.50 – 1.90

[a]From ref. 2.

E-8980

TABLE 9. – EPOXY RESIN COMPATIBILITY STUDY – LONGITUDINAL (0°) LAMINATES[a]

Material	Resin content, wt%	Specific gravity	Flexural stress, ksi	Flexural modulus, msi	Shear, ksi	Cure
AS/5208	29.3	1.59	209.5 200.3 224.5 211.4	18.7 17.9 18.8 18.4	10.7 11.2 10.0 10.6	Cure at room temperature (275° F) at 4° to 6° F per min at vacuum pressure; hold for 1 hour at 275° F; apply 85 to 100 psig and vent; 275° to 355° F at 4° to 6° F per min; hold for 2 hr at 355° F; cool to 140° F under pressure
AS/934	30.9	1.56	254.3 250.3 224.5 243.0	18.9 20.2 18.9 19.3	12.5 11.1 11.0 11.5	Cure at room temperature (250° F) at 1° to 5° F per min at vacuum pressure; hold for 15 min at 250° F; apply 100 psig and vent; hold for 45 min at 250° F; 250° to 350° F at 1° to 5° F per min; hold for 2 hr at 350° F; cool to 140° F under pressure
AS/3501	28.0	1.59	244.3 256.0 257.9 252.7	18.4 21.4 22.2 20.7	14.8 15.3 15.4 15.2	Cure at room temperature (225° F) at 2° to 3° F per min at vacuum pressure; apply 85 to 100 psig at 225° F and hold vacuum pressure; continue temperature rise to 350° F; hold at 350° F for 1/2 hr at 85 to 100 psig and vacuum; cool under pressure and vacuum to 140° F.
AS $\frac{5208}{934}$[b]	28.6	1.61	271.1 259.8 244.8 258.6	20.6 20.5 19.8 20.8	17.3 17.8 15.4 16.8	Cure at room temperature (250° F) at 3° F per min at vacuum pressure; hold for 45 min at 250° F; apply 100 psig; vent then hold for 2 hr at 355° F and 100 psi; cool under pressure and vacuum
AS $\frac{5208}{3501}$[b]	30.5	1.61	249.4 241.1 242.1 244.2	21.0 22.2 19.3 20.8	17.4 16.1 16.4 16.6	
AS $\frac{934}{3501}$[b]	29.6	1.60	260.1 255.1 253.4 256.2	20.0 19.6 19.8 19.8	15.6 14.6 17.2 15.8	

[a]From ref. 3.
[b]Alternating plies of each system.
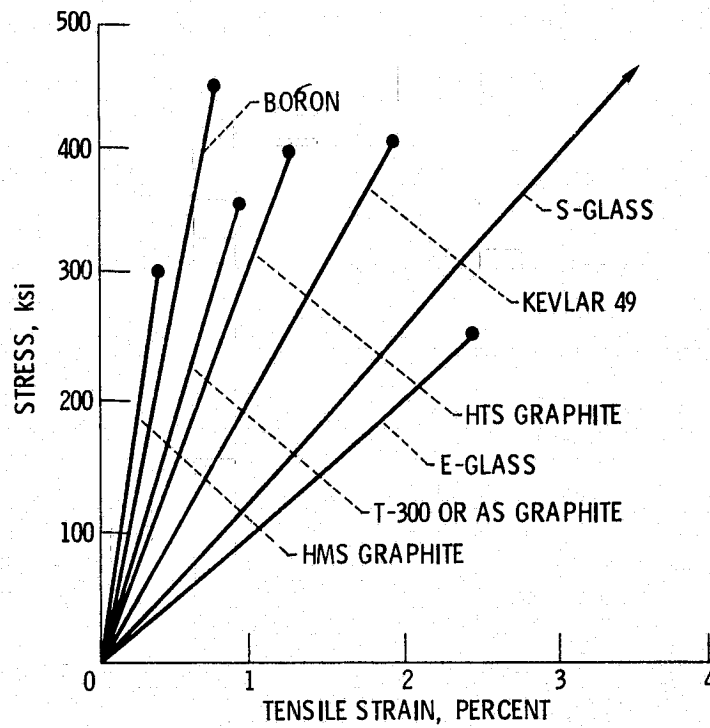
Figure 1. - Stress-strain diagrams of various fibers.
(E. I. Dupont technical data.)
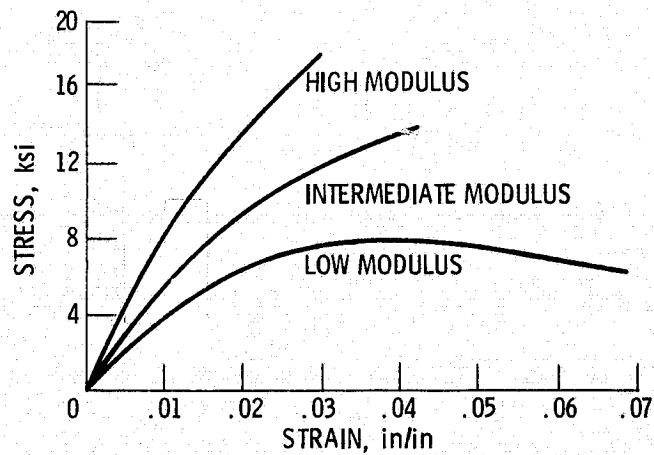
Figure 2. - Stress-strain diagrams of epoxy matrix
resins. (From ref. 1.)

| Kevlar 49 or S-glass (everywhere) |
| AS or HMS graphite |
| Kevlar 49 or S-glass |
| AS or HMS graphite |
| Kevlar 49 or S-glass |

| S-glass |
| HMS graphite |
| HMS graphite |
| HMS graphite |
| S-glass |

| S-glass |
| AS graphite |
| HMS graphite |
| AS graphite |
| S-glass |

(a-1) Interspersed.　　　　　(a-2) Core/shell.

(a) Interply.

AS or HMS graphite

S-glass

Kevlar 49
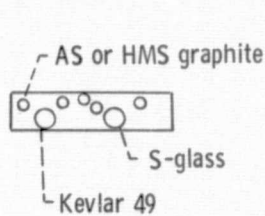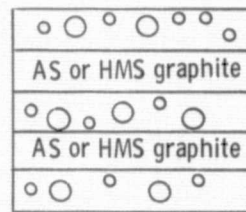
(b) Intraply.　　　　　(c-1) Interspersed.　　　　　(c-2) Core/shell.

AS or HMS graphite

AS or HMS graphite
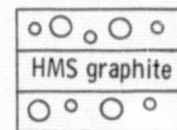
HMS graphite

(c) Interply/intraply.

Figure 3. - Cross sections of typical hybrid composites.

Ti
FM 1000
Ti (ADHESIVE)
FM 1000
B/Al
FM 1000
AS/EPOXY
FM 1000
Ti

CS-75035
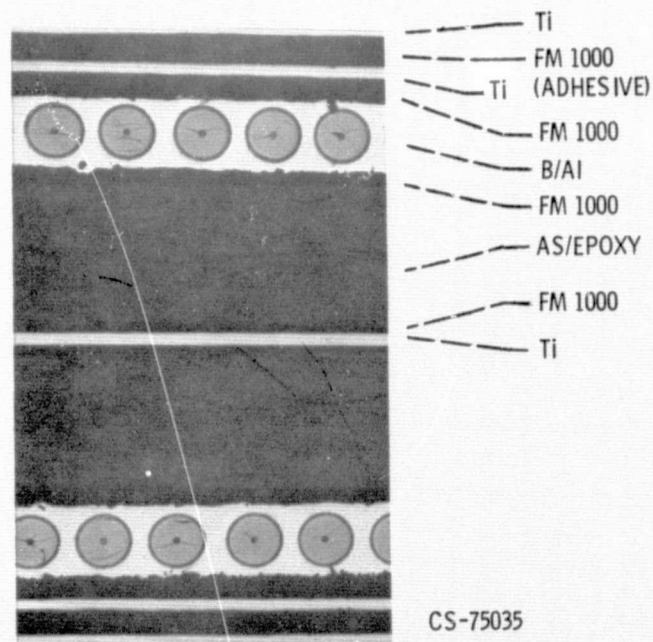
Figure 4. - Cross section of superhybrid composite (from ref.
6). X50.
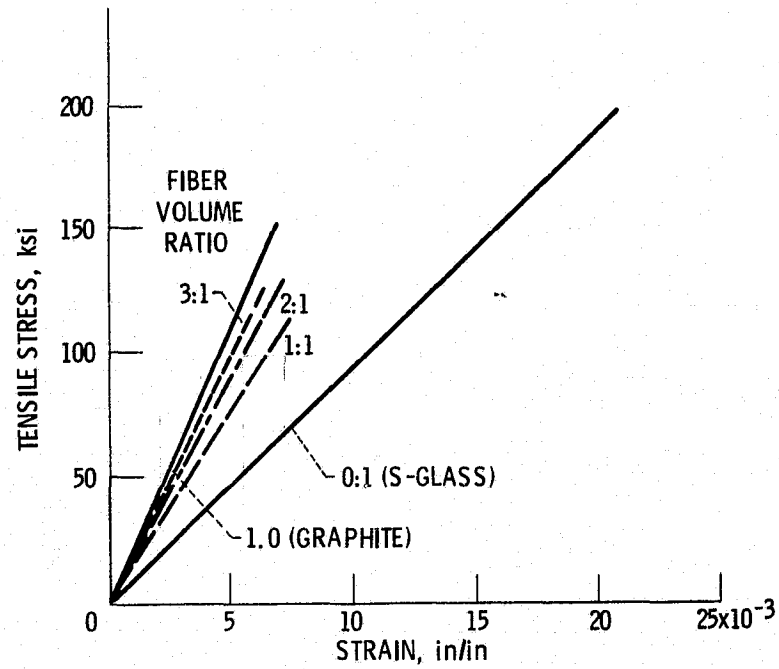
Figure 5. - Summary of tensile (0°) stress-strain diagrams for PR-286/Modmor II graphite/S-glass composites having various fiber volume ratios, compared with conventional glass and graphite composites with epoxy resin. (From ref. 4.)
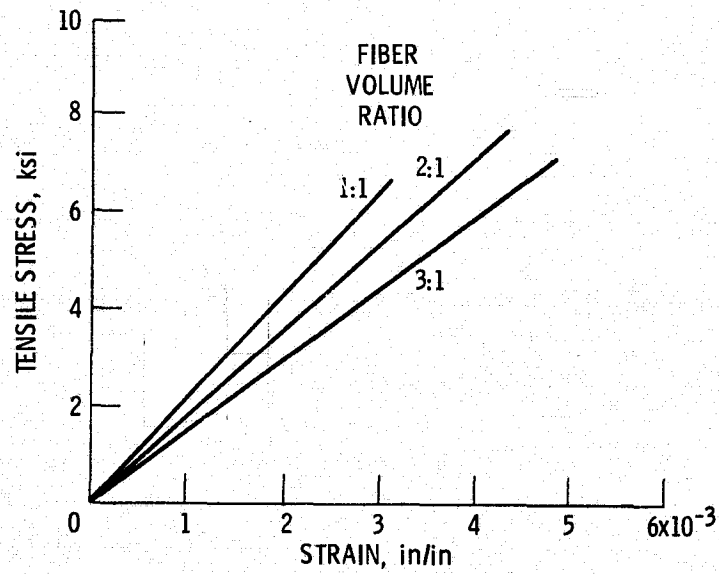
Figure 6. - Summary of tensile (90°) stress-strain diagrams for PR-286/Modmor II graphite/S-glass composites of various fiber volume ratios. (From ref. 4.)
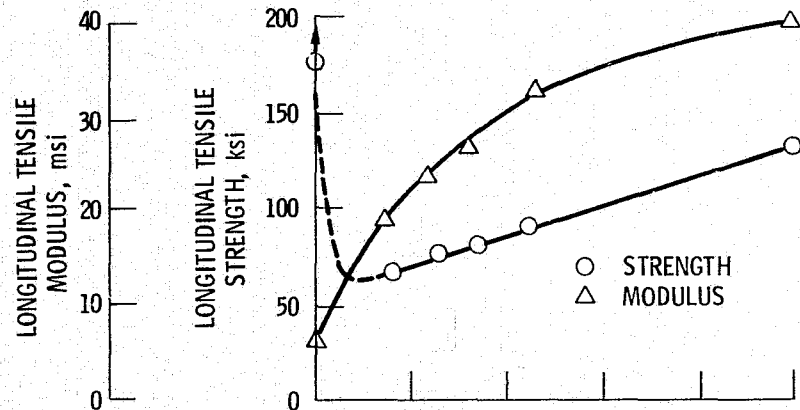
(a) LONGITUDINAL TENSILE STRENGTH AND MODULUS.
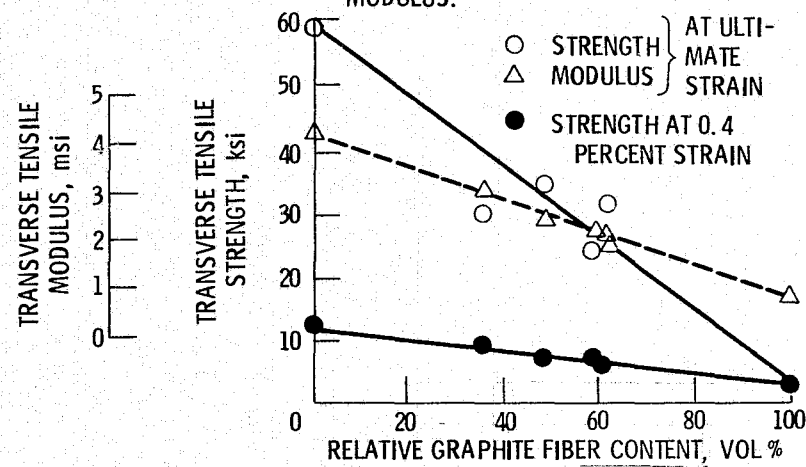
(b) TRANSVERSE TENSILE STRENGTH AND MODULUS.

(c) LONGITUDINAL COMPRESSIVE STRENGTH AND MODULUS.

(d) SHEAR STRENGTH AND MODULUS.

Figure 7. - Fracture stresses (strengths) of hybrid (GY-70 graphite/S-glass). (From ref. 7.)
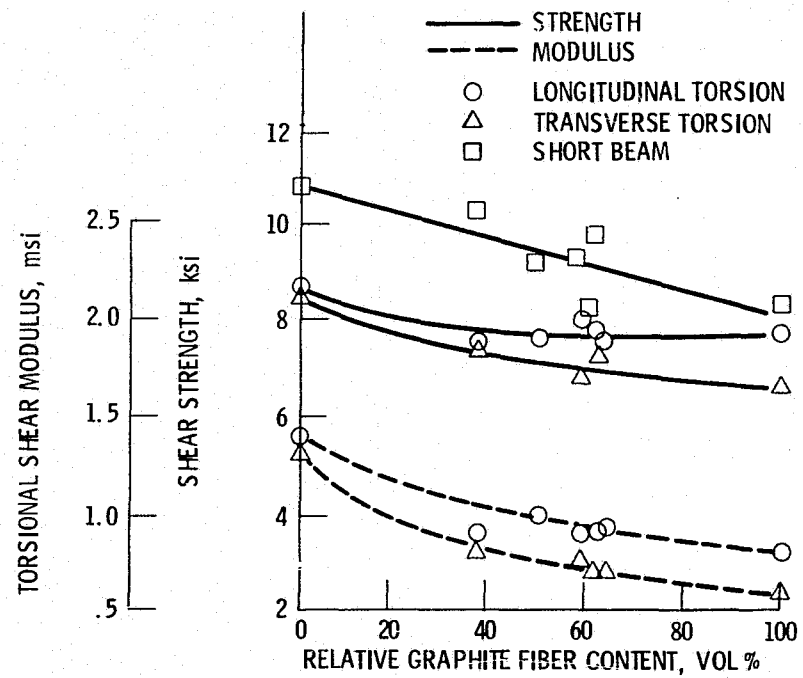
Figure 7. - Concluded.
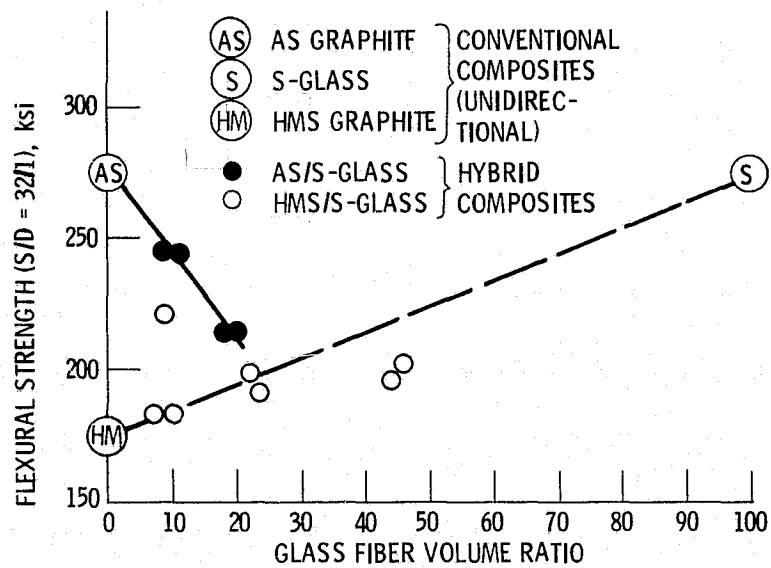
Figure 8. - Flexural strength of hybrid (AS/S-glass and HMS/S-glass) interply composites as function of glass fiber volume ratio. Span to depth ratio, S/D, 32. (From ref. 5.)
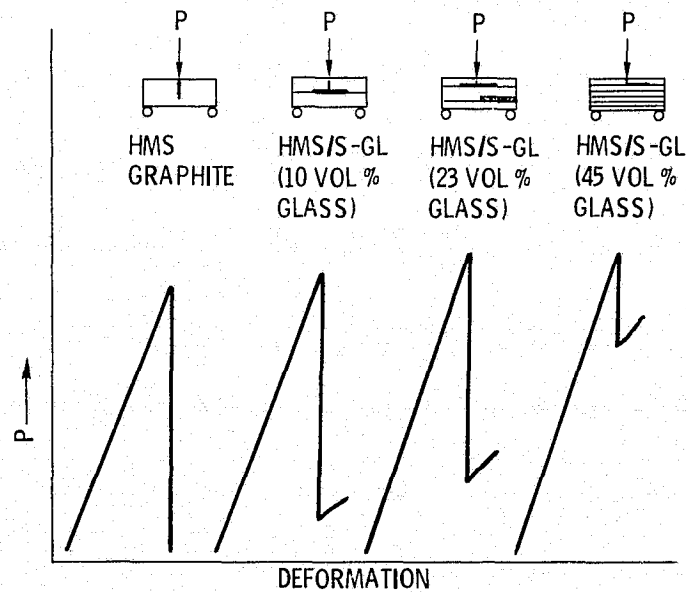
Figure 9. - Interply load deflection curve and flexural failure modes for HMS graphite and HMS graphite/S-glass with various glass contents. Span to depth ratio, S/D, 32. (From ref. 5.)
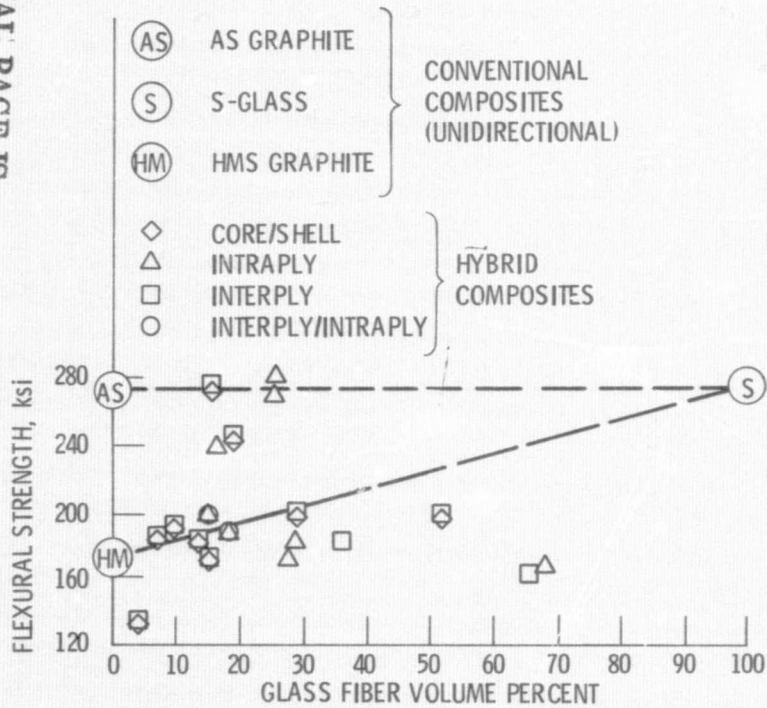
Figure 10. – Flexural strength of hybrid (AS/S-glass – HMS/
S-glass) core/shell, interply, and intraply composites as
function of glass fiber volume ratio. Span to depth ratio,
S/D, 32. (From ref. 5.)
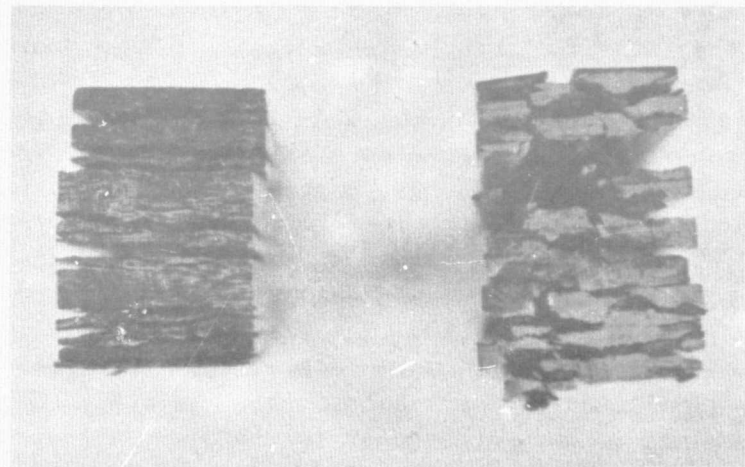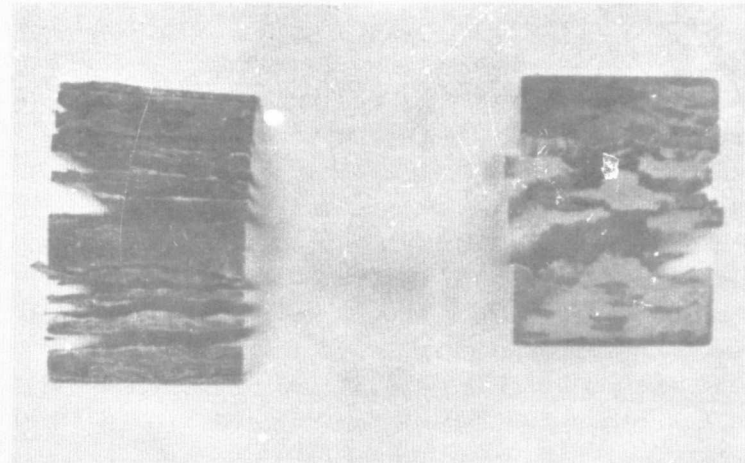
(a) INTERPLY INTERSPERSED.   (b) INTRAPLY.

Figure 11. – Fracture modes of HMS/S-glass interply and intraply hybrids
(from ref. 5).
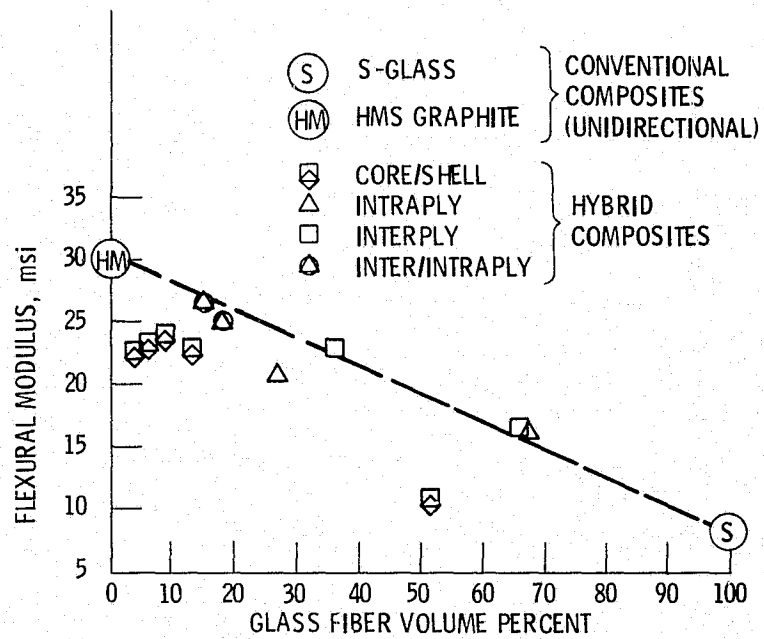
Figure 12. – Flexural modulus of hybrid (HMS/S-glass) composites as function of glass fiber volume ratio. (From ref. 5.)

Legend

——————— GRAPHITE/ EPOXY (AS/E)	
—— —— B/Al (DIFFUSION BONDED)	CONSTITUENTS
— — — B/Al (ADHESIVE BONDED)	
—·—·— Ti, B/Al	SUPERHYBRIDS
—··—··— Ti, B/Al, Gr/Ep	

STRESS, ksi

(a) LOADING PARALLEL TO FIBERS.

AXIAL STRAIN, PERCENT

(b) LOADING NORMAL TO FIBERS.
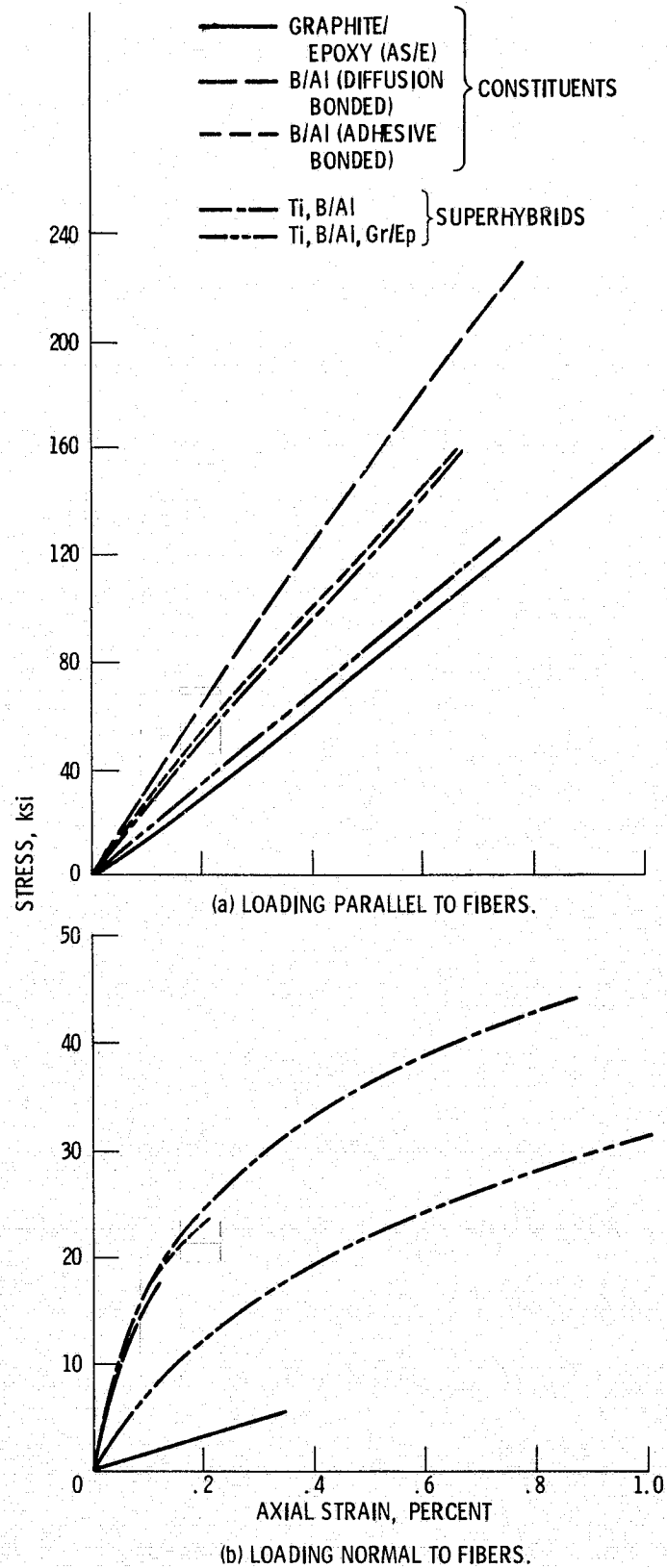
Figure 13. – Stress-strain curves for smooth tensile specimens. (From ref. 6.)
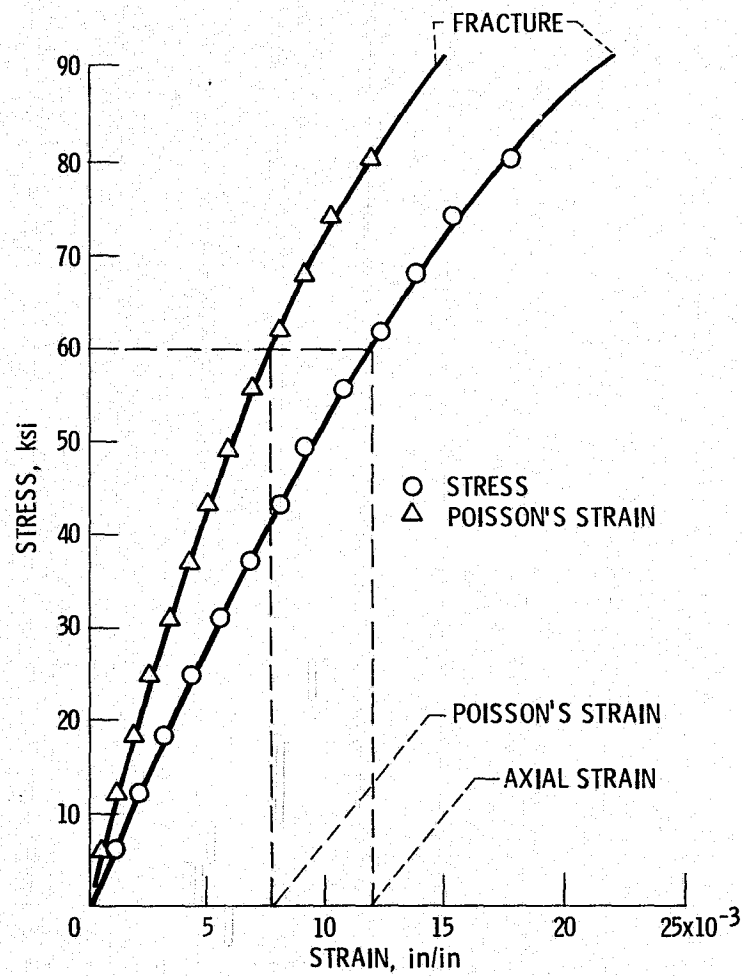
Figure 14. - Stress-strain diagrams for uniaxially loaded angleplied graphite/S-glass/epoxy hybrid composite $(\pm 45^0/0^0)_s$. Load parallel to 0^0 direction. (From ref. 8.)
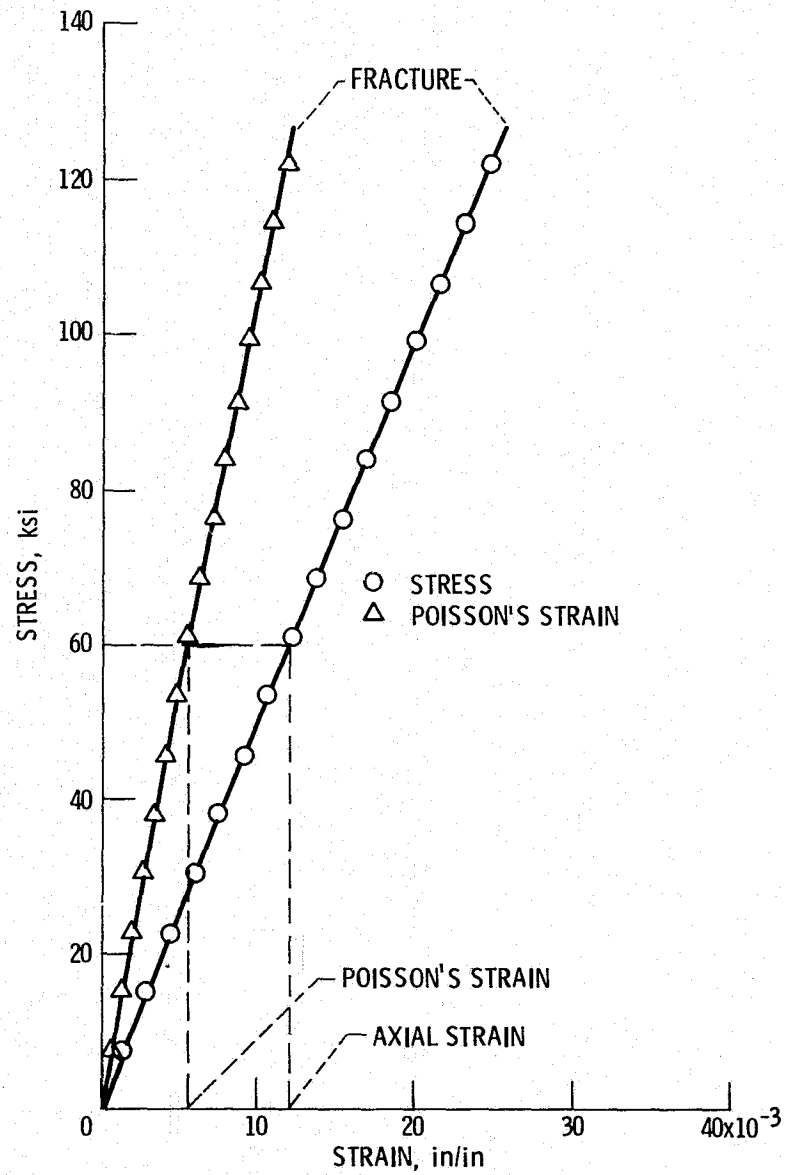
Figure 15. - Stress-strain diagrams for uniaxially load angle-plied Kevlar 49/S-glass/epoxy hybrid composite $(\pm 45^0/0^0_4)_s$. (From ref. 8.)
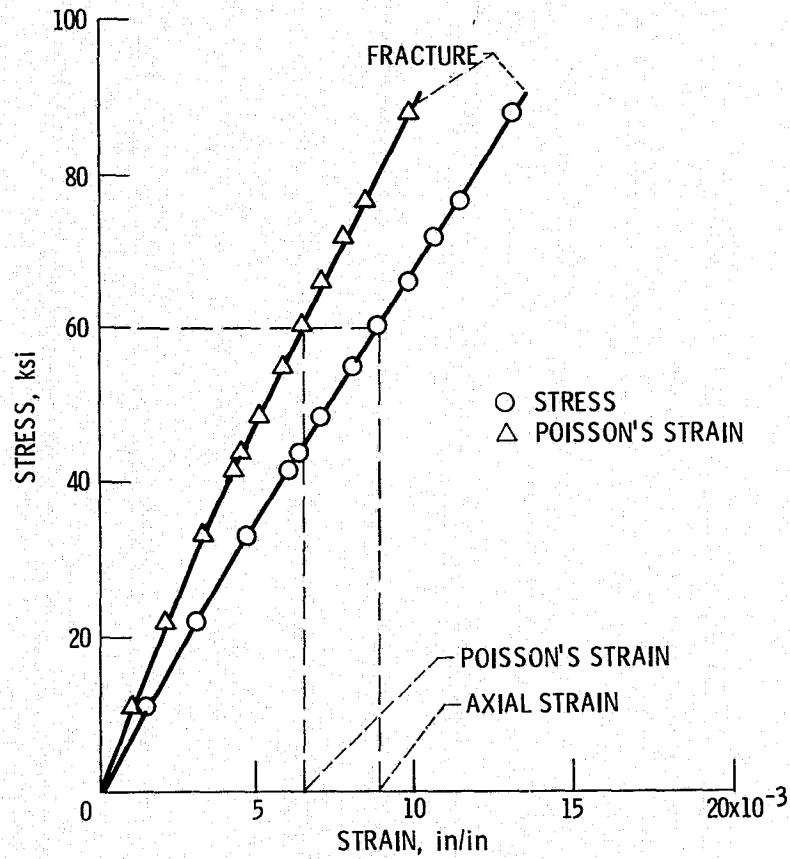
Figure 16. - Stress-strain diagrams for uniaxially loaded angleplied HM graphite/Kevlar 49/epoxy hybrid composite $\left(\pm 45^0/0^0_2\right)_s$. (From ref. 8.)
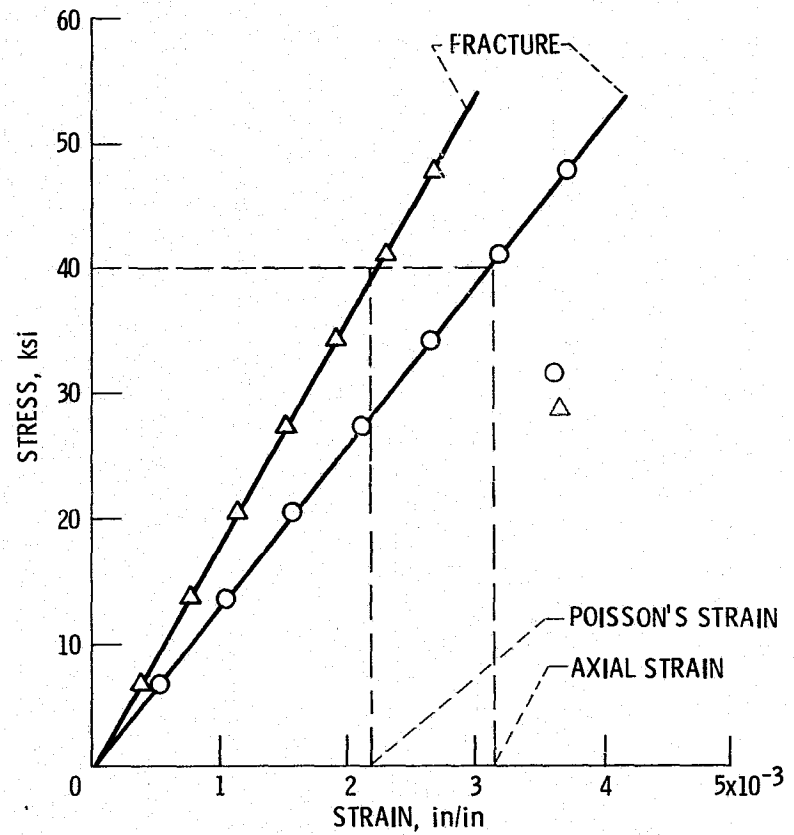
Figure 17. - Stress-strain diagrams for uniaxially loaded HM graphite/Kevlar 49/epoxy angleplied hybrid composite $\left(\pm 45^0/0^0/0^0\right)_s$. (From ref. 9.)
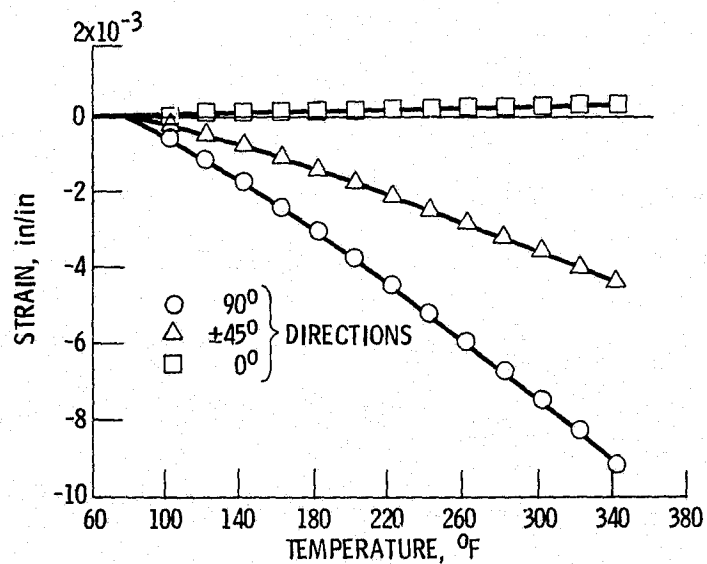
Figure 18. - Restrained strains in longitudinal (0^0)
Kevlar 49 plies of (0^0 Kev/$\pm 45^0$ Gr/0^0 Gr)$_s$ and ($\pm 45^0$
Gr/0^0 Kev/0^0 Gr)$_s$ HM graphite/Kevlar 49/epoxy hybrid
composites. (From ref. 10.)
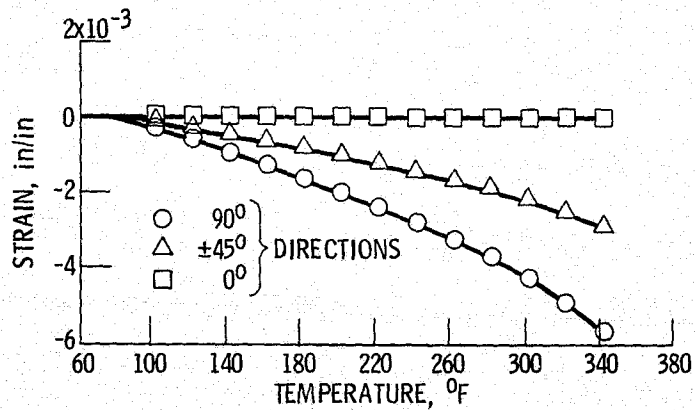
Figure 19. - Restrained strain in longitudinal (0^0)
graphite plies of (0^0 Kev/$\pm 45^0$ Gr/0^0 Gr)$_s$ and ($\pm 45^0$
Gr/0^0 Kev/0^0 Gr)$_s$ HM graphite/Kevlar 49/epoxy hybrid
composites. (From ref. 10.)
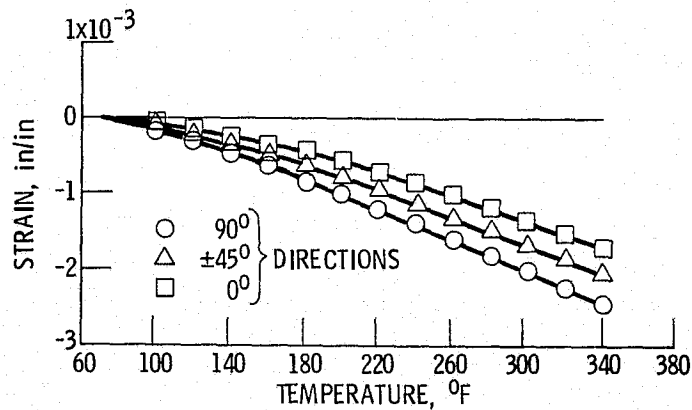
Figure 20. - Restrained strains in longitudinal (0^0) S-glass plies of (0^0 S-GL/±45^0 Gr/0^0 Gr)$_s$ and (±45^0 Gr/0^0 S-GL/0^0 Gr)$_s$ HM graphite/S-glass/epoxy hybrid composites. (From ref. 10.)
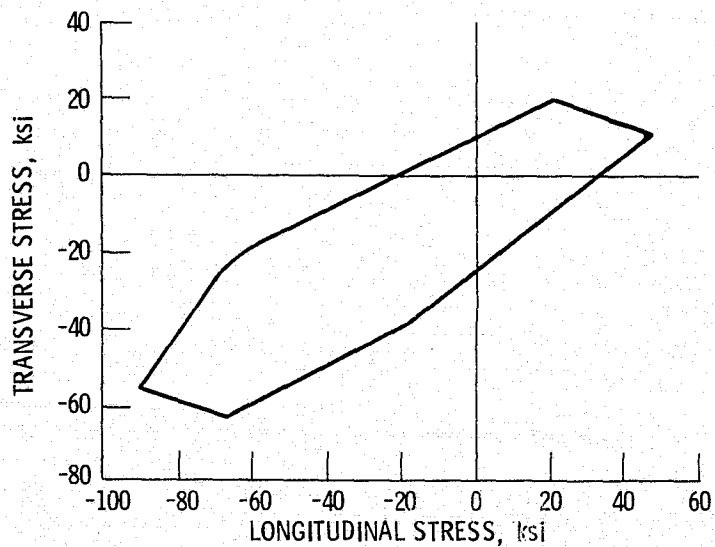
Figure 21. - Interaction diagram for S-glass/boron hybrid composite $(0^0_3/±45^0)_s$. (From ref. 19.)
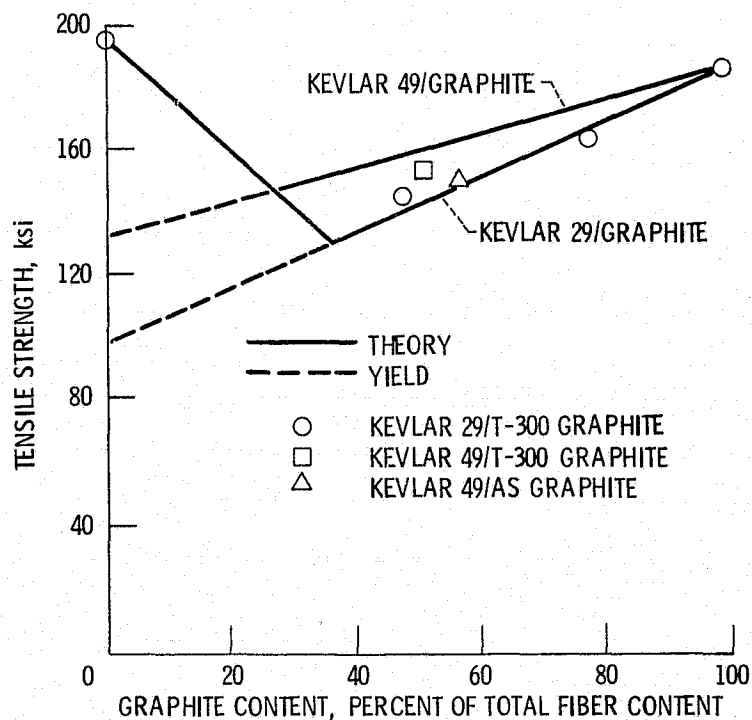
Figure 22. - Tensile strength of Kevlar/graphite interply
unidirectional hybrid composites compared with theoret-
ical prediction. Total fiber content, 60 vol %. (From
ref. 24.)
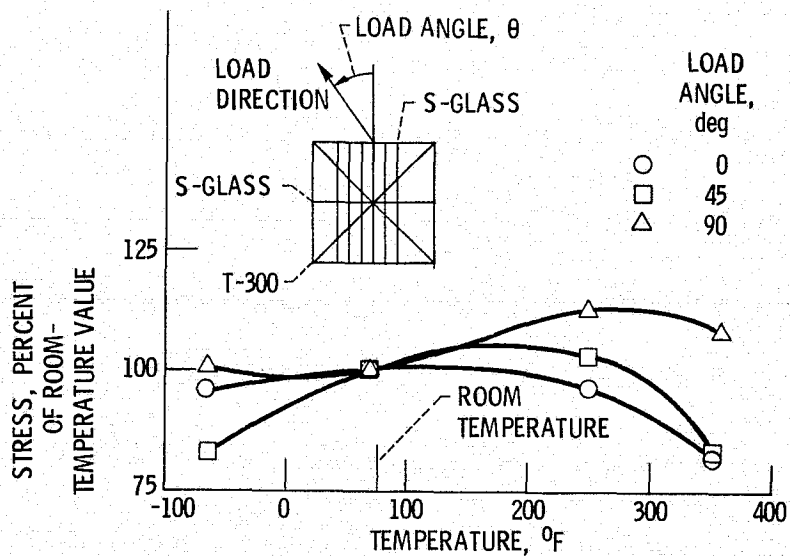
Figure 23. - Tensile fracture stress of S-glass/T-300/
S-glass/S-glass hybrid composite $(0^0_3/\pm45^0/90^0/0^0_3)_s$
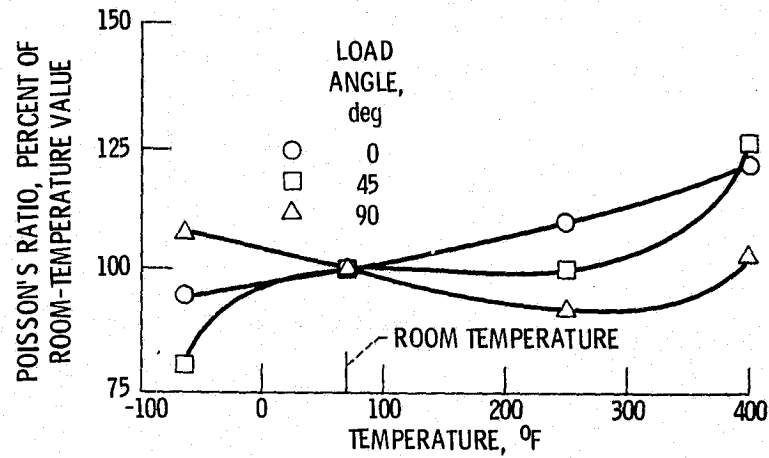as function of temperature. (From ref. 2.)
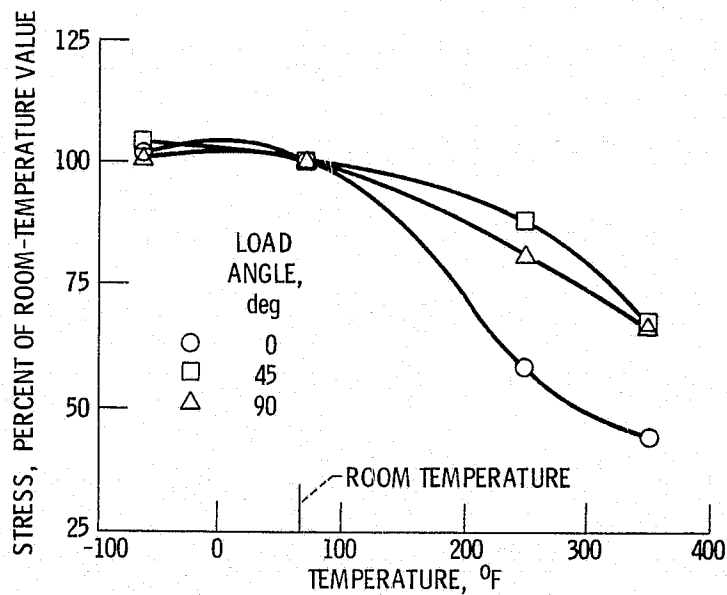
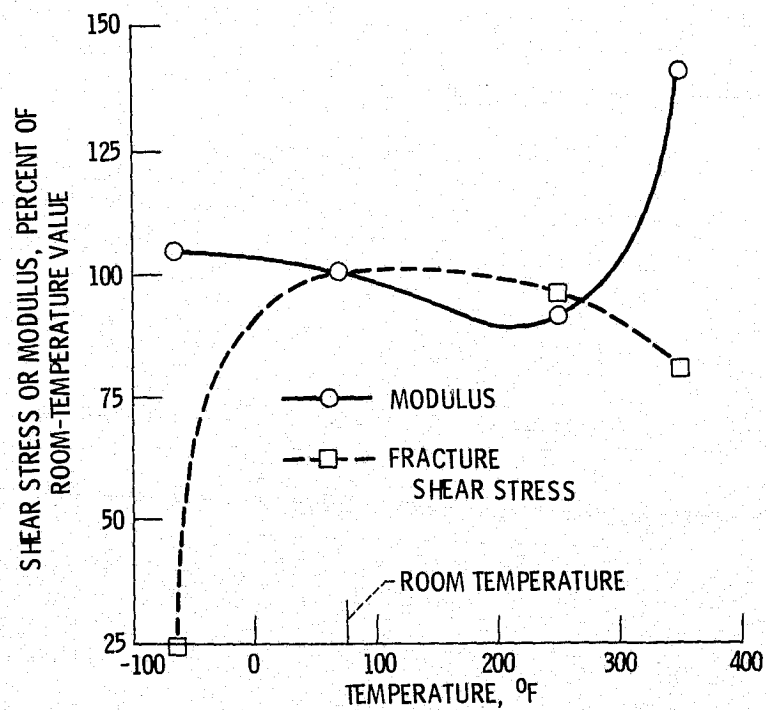Figure 24. – Compression fracture stress of S-glass/
T-300/S-glass/S-glass hybrid composite $\left(0^0_3/\pm45^0/90^0/0^0_3\right)_s$
as function of temperature. (From ref. 3.)
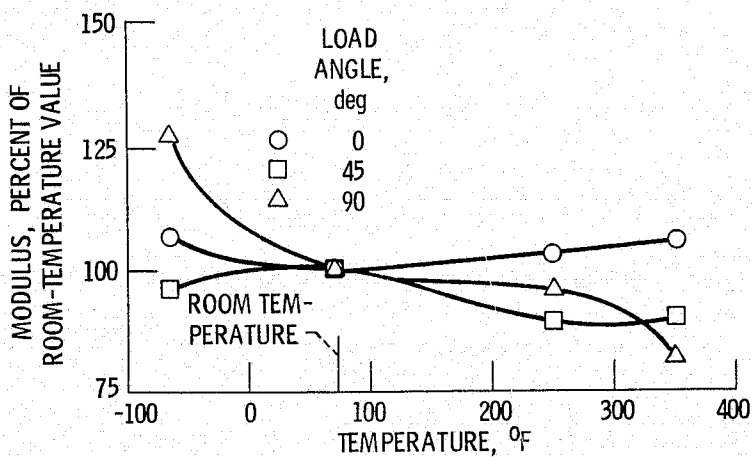
Figure 25. – Tensile fracture modulus of S-glass/T-300/
S-glass/S-glass hybrid composite $\left(0^0_3/\pm45^0/90^0/0^0_3\right)_s$ as
function of temperature. (From ref. 2.)

Figure 26. - Poisson's ratio of S-glass/T-300/S-glass/
S-glass hybrid composite $(0_3^0/\pm 45^0/90^0/0_3^0)_s$ as function
of temperature. (From ref. 2.)

Figure 27. - Fracture shear stress and modulus for
S-glass/T-300/S-glass/S-glass hybrid composite
$(0_3^0/\pm 45^0/90^0/0_3^0)_s$ as function of temperature. Load
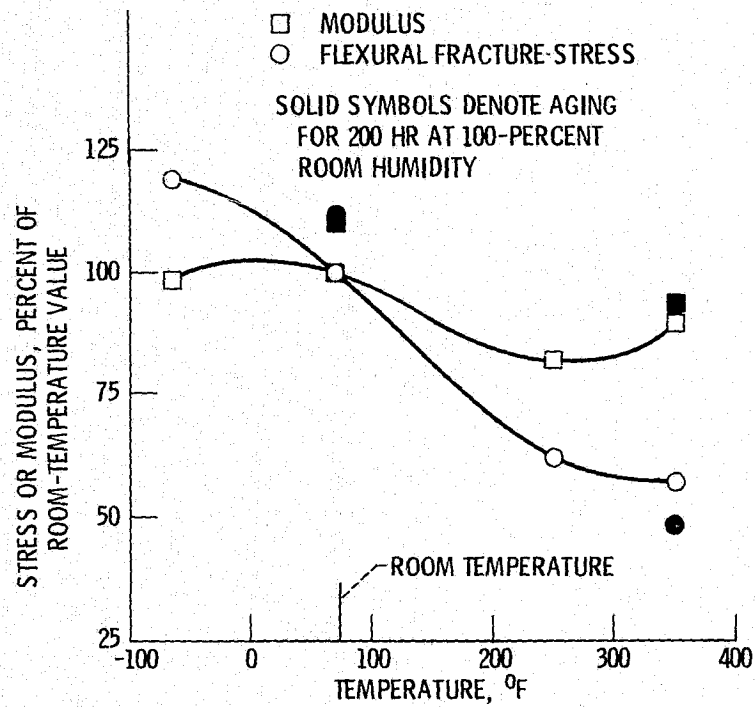angle, 0^0. (From ref. 2.)

Figure 28. - Flexural fracture stress and modulus for
S-glass/T-300/S-glass/S-glass hybrid composite
$\left(0_3^0/\pm 45^0/90^0/0_3^0\right)_s$ as function of temperature and
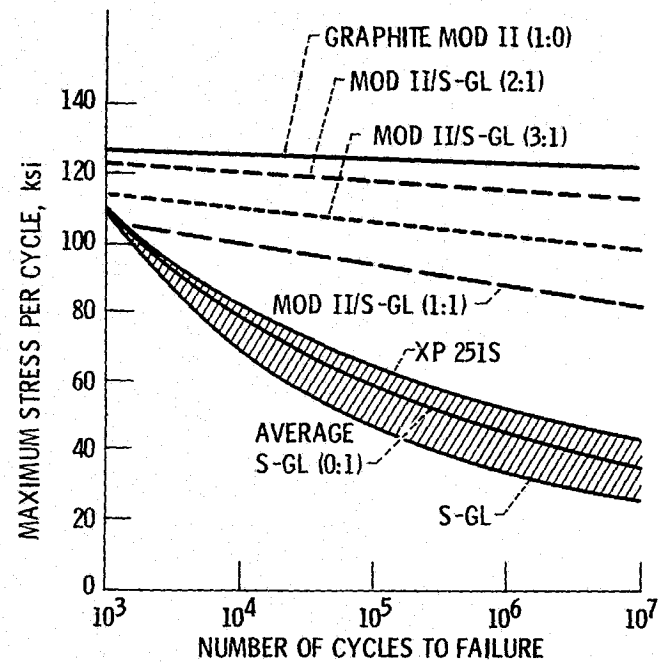moisture content. (From ref. 2.)

Figure 29. - Tensile fatigue lives of unidirectional
hybrid composites and constituents. Fiber orien-
tation, 0^0; stress ratio, 0.1; cycling frequency,
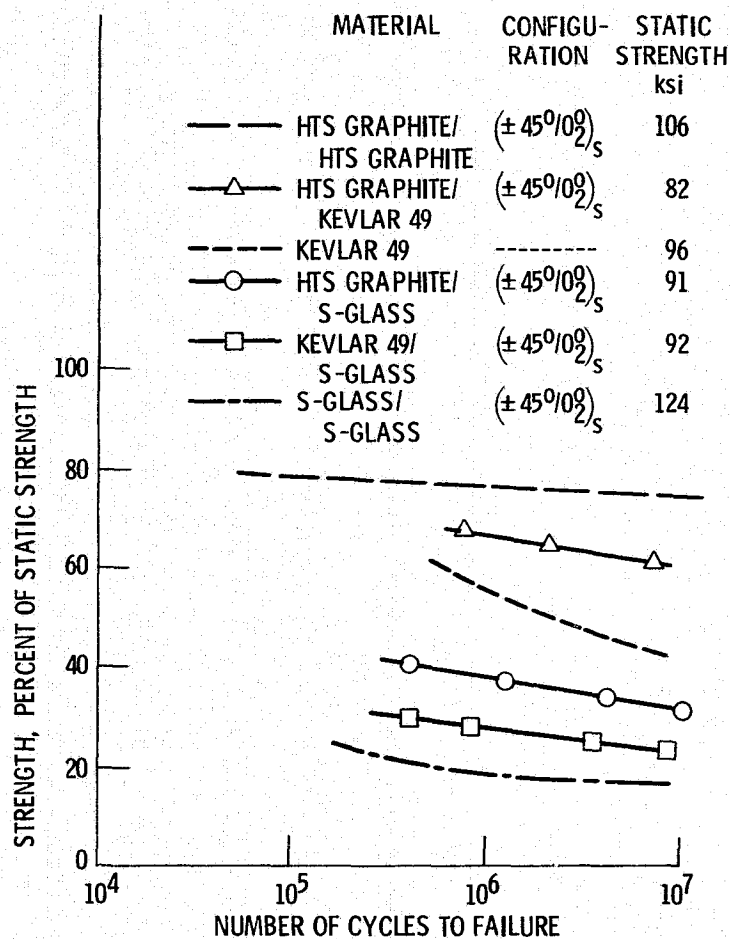1800 Hz; test temperature, room temperature.
(From ref. 4.)

MATERIAL	CONFIGU-RATION	STATIC STRENGTH ksi
——— HTS GRAPHITE/ HTS GRAPHITE	$(\pm 45^0/0^0_2)_s$	106
—△— HTS GRAPHITE/ KEVLAR 49	$(\pm 45^0/0^0_2)_s$	82
————— KEVLAR 49	————	96
—○— HTS GRAPHITE/ S-GLASS	$(\pm 45^0/0^0_2)_s$	91
—□— KEVLAR 49/ S-GLASS	$(\pm 45^0/0^0_2)_s$	92
——— S-GLASS/ S-GLASS	$(\pm 45^0/0^0_2)_s$	124

Figure 30. - Tensile fatigue lives of angleplied hybrid composites and constituents. Stress ratio, 0.1; cycling frequency, 5 and 30 Hz; test temperature, room temperature. (From ref. 8.)

○ T-300/Kev 49-181/T-300/T-300 $(0^0_2/45^0_2/90^0/0^0_2)_s$

□ S-GL/T-300/S-GL/S-GL $(0^0_3/\pm 45^0/90^0/0^0_3)_s$

OPEN SYMBOLS DENOTE NO AGING
SOLID SYMBOLS DENOTE AGING FOR
500 CYCLES AT 65° TO 300° F
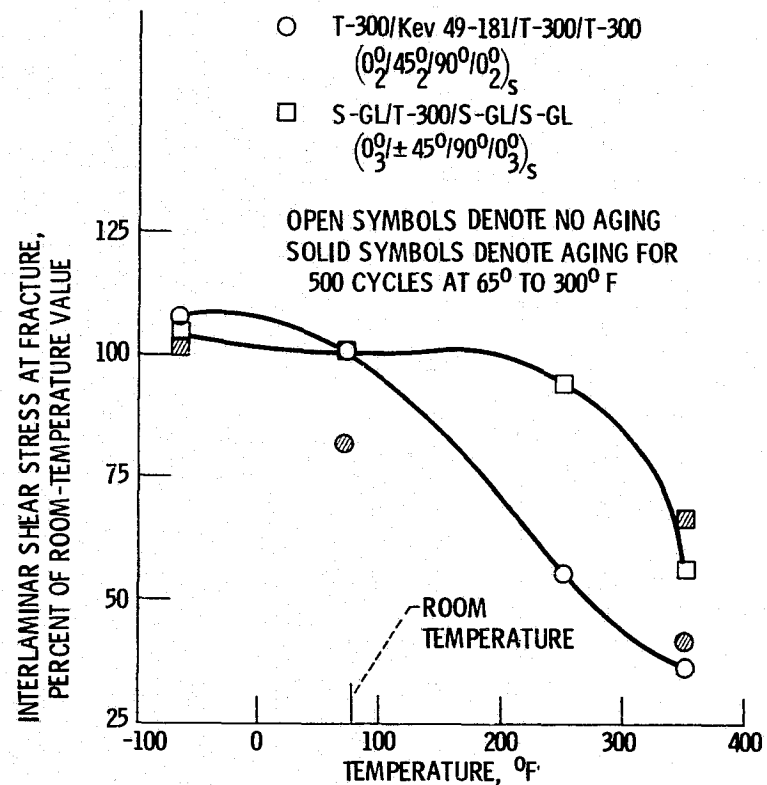
Figure 31. - Interlaminar shear stress at fracture (short beam) for hybrid composites as function of thermal cycling and temperature. (From ref. 2.)
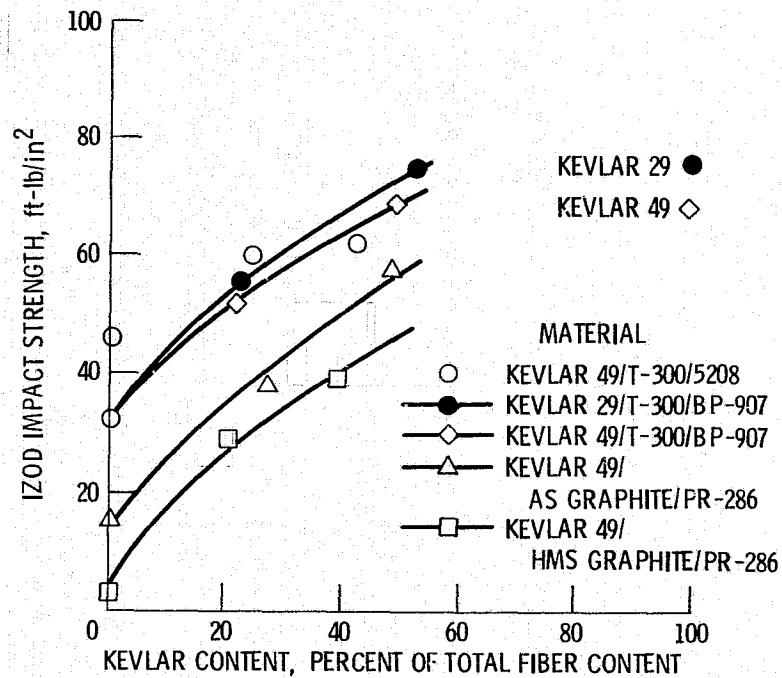
Figure 32. – Izod impact strength of unidirectional Kevlar hybrid composites. Total fiber content, 60 vol %. (From ref. 24.)
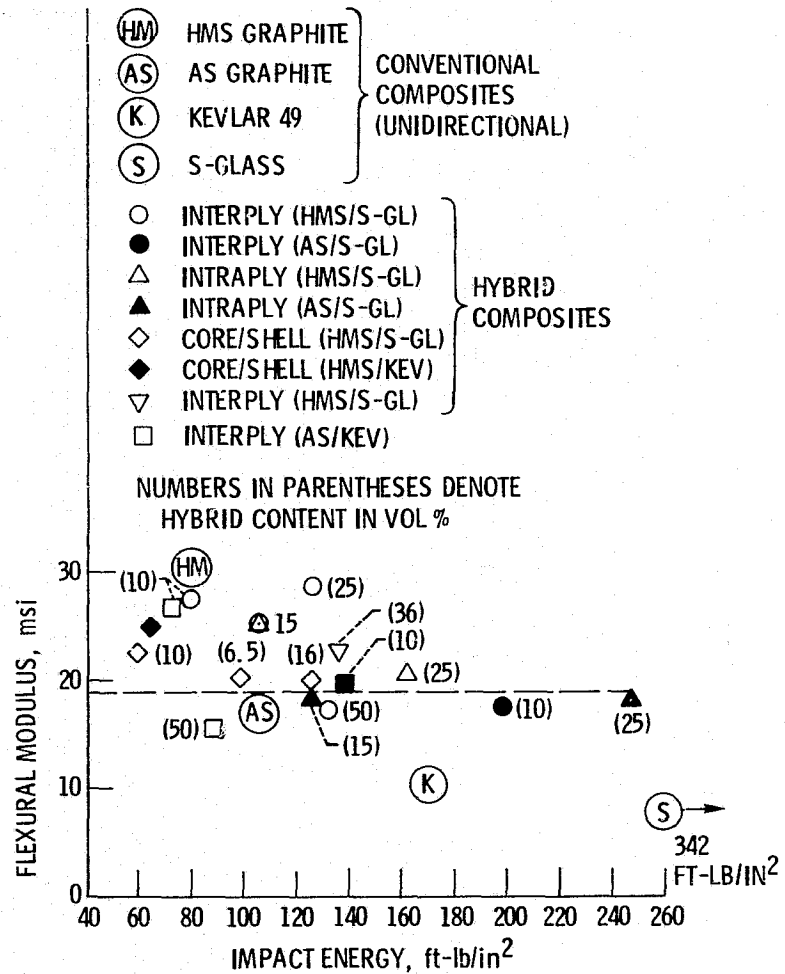

Figure 33. – Flexural modulus as function of pendulum impact per unit area for unidirectional hybrid fiber/epoxy composites. (From ref. 5.)
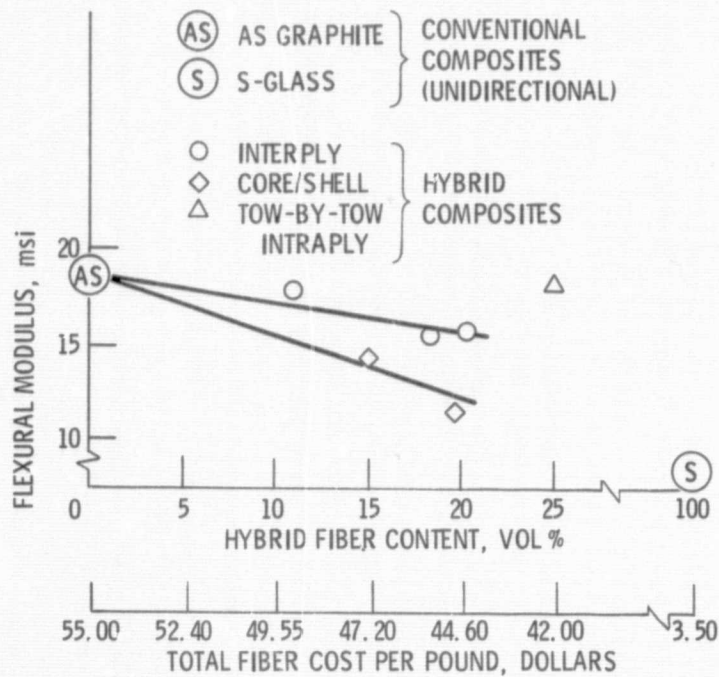
Figure 34. - Flexural behavior/cost trade-off for AS graphite/
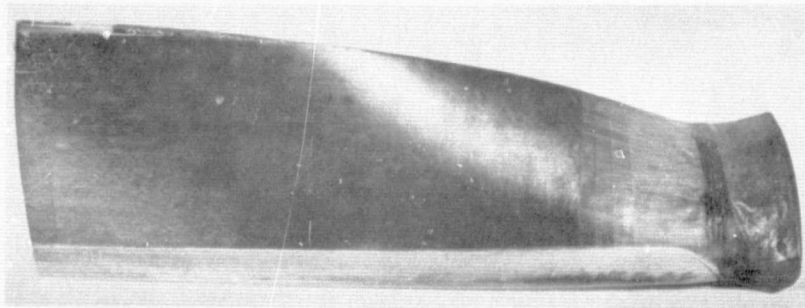S-glass composites. (From ref. 5.)

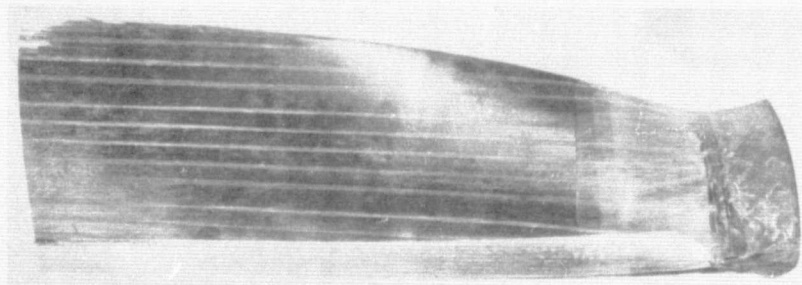Figure 35. - Interply hybrid composite compressor blade (from ref. 46).

Figure 36. - Intraply hybrid composite compressor blade (from ref. 46).